Biomaterials 31 (2010) 7150–7166

Contents lists available at ScienceDirect

Biomaterials

journal homepage: www.elsevier.com/locate/biomaterials

Degradable, pH-sensitive, membrane-destabilizing, comb-like polymers for intracellular delivery of nucleic acids

Yen-Ling Lin [a,1], Guohua Jiang [a,1], Lisa K. Birrell [a], Mohamed E.H. El-Sayed [a,b,*]

[a] University of Michigan, College of Engineering, Department of Biomedical Engineering, Cellular Engineering & Nano-Therapeutics Laboratory, Ann Arbor, MI, 48109, USA
[b] University of Michigan, Macromolecular Sciences & Engineering Program, Ann Arbor, MI, 48109, USA

ARTICLE INFO

Article history:
Received 22 April 2010
Accepted 19 May 2010
Available online 25 June 2010

Keywords:
pH-sensitive polymers
Acid-labile linkage
Comb-like polymers
Endosomal escape
Intracellular siRNA delivery

ABSTRACT

This report describes the design and synthesis of a new series of degradable, pH-sensitive, membrane-destabilizing, comb-like polymers that can enhance the intracellular delivery of therapeutic nucleic acids. These comb-like polymers are based on a diblock polymer backbone where the first block is a copolymer of pH-sensitive ethyl acrylic acid (EAA) monomers and hydrophobic butyl methacrylate (BMA) or hexyl methacrylate monomers. The second block is a homopolymer of *N*-acryloxy succinimide (NASI) or ß-benzyl L-aspartate *N*-carboxy-anhydride (BLA-NCA) monomers, which are functionalized to allow controlled grafting of hydrophobic HMA and cationic trimethyl aminoethyl methacrylate (TMAEMA) copolymers via acid-labile hydrazone linkages. These comb-like polymers displayed high hemolytic activity in acidic solutions, which increased with the increase in polymer concentration. All comb-like polymers degraded into small fragments upon incubation in an acidic solution (pH 5.8) due to hydrolysis of the hydrazone linkages connecting the hydrophobic/cationic grafts to the polymer backbone. Comb-like polymers successfully complexed anti-GAPDH siRNA molecules into serum- and nuclease-stable particles, which successfully silenced GAPDH expression at both the mRNA and protein levels. These results collectively indicate the potential of these new comb-like polymers to serve as vehicles for effective intracellular delivery of therapeutic nucleic acids.

1. Introduction

Recent advances in drug design have led to the development of several classes of nucleic acid molecules such as plasmid DNA (pDNA), antisense oligodeoxynucleotides (ASODN), short interfering RNA (siRNA), and micro RNA (miRNA), which have the potential to treat cancer, viral infection, and cardiovascular and neurodegenerative diseases [1–5]. These nucleic acid therapies are typically internalized by endocytosis where they accumulate in the endosomal-lysosomal trafficking pathway, which results in their degradation and loss of therapeutic activity [6,7]. Transforming these nucleic acid molecules into therapeutic agents with defined dosing regimens and well-characterized activity requires the development of specialized carriers that can successfully condense and shield nucleic acid molecules into nano-sized particles that preferentially accumulate in the diseased tissue, selectively taken up by target cells, effectively escape the endosomal compartment, and deliver their therapeutic cargo into the cytoplasm to interact with defined intracellular targets and produce the desired therapeutic activity [8–11].

Viral vectors proved to be highly efficient in delivering nucleic acids into the cytoplasm of infected cells [12]. For example, the influenza virus utilizes the pH-sensitive membrane-destabilizing Hemagglutinin protein displayed on the viral coat to disrupt the endosomal membrane and enter the cytoplasm [13–17]. Hemagglutinin and other fusion proteins are characterized by their unique ability to switch from an ionized and hydrophilic conformation at physiologic pH to a hydrophobic and membrane-active one in response to acidic endosomal pH gradients, which destabilizes the endosomal membrane leading to leakage of endosomal contents into the cytoplasm [13–17]. Szoka, Wagner, and others have used artificial, pH-sensitive, fusogenic peptides to enhance cytoplasmic gene delivery [18–26]. Despite the endosomolytic activity of these fusogenic peptides, their potential immunogenicity and toxicity limit their clinical use.

Several groups have focused their efforts on the development of synthetic polymeric carriers that mimic the endosomolytic properties

* Corresponding author. University of Michigan, Department of Biomedical Engineering, 1101 Beal Avenue, Room 2150, Lurie Biomedical Engineering Building, Ann Arbor, MI 48109, United States. Tel.: +1 734 615 9404; fax: +1 734 647 4834.
E-mail address: melsayed@umich.edu (M.E.H. El-Sayed).
URL: http://www.bme.umich.edu/centlab.php
[1] These authors contributed equally to this research work.

0142-9612/$ – see front matter © 2010 Elsevier Ltd. All rights reserved.
doi:10.1016/j.biomaterials.2010.05.048

of fusogenic proteins and enhance the cytoplasmic delivery of therapeutic macromolecules [27,28]. These polymers are characterized by their unique ability to "sense" the changes in environment pH where they undergo a change from a hydrophilic, stealth-like conformation at physiologic pH to a hydrophobic and membrane-destabilizing one in response to acidic endosomal pH gradients. Poly(ethylacrylic acid) (PEAA) is the first reported polymer to display a pH-dependent disruption of synthetic lipid vesicles at acidic pH of 6.3 or lower [29,30]. Stayton, Hoffman, and coworkers expanded this family of synthetic polymers by synthesizing poly(propylacrylic acid) (PPAA) and copolymers of acrylic acid and alkyl acrylates, which showed a pH-dependent membrane-destabilizing activity that increased with the increase in the proportion of hydrophobic alkyl acrylates in polymer composition [31,32]. PPAA exhibited a pH-dependent membrane-destabilizing activity that is one order of magnitude higher than PEAA [31,32] and proved to enhance the transfection efficiency of cationic lipid/pDNA complexes both *in vitro* [33,34] and *in vivo* [35]. However, the number of anionic carboxylate groups of the PPAA polymer affects charge balance in cationic lipid and polymer/DNA complexes and the order of mixing of PPAA proved to affect the size, surface charge, stability, and transfection efficiency of these complexes [33,36]. Subsequent polymers incorporated a glutathione-sensitive monomer, pyridyl disulfide acrylate (PDSA), to allow direct coupling of cationic peptides to the pH-sensitive polymer backbone [37,38]. These polymer-peptide conjugates proved to complex DNA nucleotides and retain their membrane-destabilizing activity in response to acidic pH gradients [37,38].

Earlier research showed that the membrane-destabilizing activity and the ability of these polymers to condense DNA/RNA molecules relies on a delicate balance between the content of pH-sensitive acrylic acid and hydrophobic alkyl acrylate monomers, the net positive charge of polymer-cationic peptide conjugates, and their overall molecular weight [38]. The optimum molar content of EAA and PAA monomers is typically more than 60% of the polymer backbone to maintain aqueous solubility and pH sensitivity of the polymer. However, this high content of anionic carboxylate groups causes electrostatic repulsion between the pH-sensitive polymer and the negatively charged phosphate groups of the loaded DNA/RNA molecules, which reduces the amount of nucleic acid incorporated in cationic lipid or polymer/DNA complexes [38]. Covalent conjugation of cationic peptides to PDSA-containing polymers significantly improved their aqueous solubility and allowed for effective complexation of DNA/RNA molecules [37,38]. However, PDSA content in these polymers remains limited to avoid reducing the content of the hydrophobic alkyl acrylate monomers in the polymer backbone, which are essential to achieve the desired membrane-destabilizing activity [37,38]. The membrane-destabilizing activity of these polymers increases with the increase in polymer's molecular weight. However, these are linear non-degradable polymers that rely on renal excretion to be eliminated from the body, which limits their molecular weight to a maximum of 45–50 kDa [38].

This research focuses on the design and synthesis of polymeric carriers that can condense a large dose of therapeutic nucleic acids into particles that can "sense" the drop in environment pH after internalization into target cells via endocytosis, which will trigger particle degradation into small membrane-destabilizing polymer fragments that rupture the endosomal membrane and release the encapsulated nucleic acid cargo into the cytoplasm to interact with their targets and produce the desired therapeutic activity (Fig. 1). These comb-like polymers are constructed on diblock copolymers where the first block incorporates pH-sensitive EAA monomers and hydrophobic butyl methacrylate (BMA) or hexyl methacrylate (HMA) monomers at a 60/40 M feed ratio. The second block is synthesized using *N*-acryloxy succinimide (NASI) or ß-benzyl L-aspartate *N*-carboxy-anhydride (BLA-NCA) monomers, which are functionalized to allow for controlled grafting of hydrophobic HMA and cationic trimethyl aminoethyl methacrylate (TMAEMA) copolymers at a 50/50 M feed ratio via acid-labile hydrazone linkages (Fig. 2).

The polymer backbone is tailored to have a molecular weight below 45–50 kDa and to exhibit a high membrane-destabilizing activity in response to acidic stimuli. The comb-like grafts have an average molecular weight of 20 kDa per graft and incorporate cationic TMAEMA monomers for condensation of DNA/RNA molecules and hydrophobic HMA monomers to enhance their membrane-destabilizing activity. These comb-like polymers will complex nucleic acid molecules via electrostatic interaction forming pH-sensitive particles that will fragment upon exposure to acidic endosomal pH gradients due to hydrolysis of the hydrazone linkages connecting poly(HMA-*co*-TMAEMA) grafts to the polymers backbone (Fig. 3). The membrane-destabilizing backbone and the hydrophobic monomers embedded in the comb-like grafts will synergistically disrupt the endosomal membrane and release the nucleic acid cargo into the cytoplasm to produce the desired therapeutic activity. These polymer fragments are engineered to be quickly eliminated *in vivo* by renal excretion.

This manuscript describes the synthesis, characterization, and membrane-destabilizing activity of a new family of degradable, pH-sensitive, comb-like polymers. It describes the ability of these comb-like polymers to condense siRNA molecules into particles and reports their size, zeta potential, and serum and nuclease stability. We also report the uptake of particles incorporating anti-GAPDH siRNA molecules into MCF-7 breast cancer cells and the associated knockdown of GAPDH gene expression as a function of particle composition.

2. Materials and methods

2.1. Materials

Copper (I) bromide (Cu(I)Br), 1,1,4,7,7-pentamethyldiethylenetriamine (PMDETA), 2,2′-Azo-bis(isobutyronitrile) (AIBN), BMA, HMA, NASI, TMAEMA, and all solvents were purchased from Sigma–Aldrich Chemical Co. (St. Louis, MO). All reagents were used as delivered without further purification except for AIBN, which was crystallized from methanol prior to use. EAA monomer and 2-dodecylsulfanylthiocarbonylsulfanyl-2-methyl propionic acid (DMP) chain transfer agent were synthesized following published procedures [39,40]. The ß-benzyl L-aspartate *N*-carboxy-anhydride (BLA-NCA) monomer was synthesized using triphosgene following the Fuchs-Farthing method [41]. The human anti-GAPDH siRNA, FAM-labeled anti-GAPDH siRNA, negative siRNA sequence, kDalert GAPDH assay kit, RNase V1 enzyme, and siPORT-NH_2 transfection reagent were purchased from Ambion Inc. (Austin, TX). The RNeasy Mini Kit and Omniscript reverse transcriptase kit were purchased from Qiagen (Valencia, CA). The TaqMan universal PCR master mix and TaqMan gene expression assays for human GAPDH and β-actin genes were purchased from Applied Biosystems (Foster, CA). The PicoGreen assay was purchased from Molecular probes (Eugene, OR).

2.2. Synthesis of poly(ethyl acrylic acid-co-alkyl methyl acrylate) copolymers

The first block of the polymer backbone was synthesized by reversible addition-fragmentation chain transfer (RAFT) polymerization (Fig. 4A) and random free radical polymerization (Fig. 5A). For synthesis following RAFT polymerization techniques, we mixed EAA monomers (1.0 gm, 10×10^{-3} mol) with BMA monomers (3.3×10^{-3} mol), DMP (33 mg, 9.15×10^{-5} mol), and AIBN (3 mg, 1.83×10^{-5} mol) in a 50 ml round bottom Schlenk tube. The reaction mixture was degassed by purging with nitrogen for 20 min and placed in an oil bath at 60 °C for 17 h. The resulting crude polymer was dissolved in dimethyl formamide (DMF), precipitated in diethyl ether, and dried under vacuum to yield pure poly(EAA-*co*-BMA) polymer. For synthesis using random free radical polymerization, we replaced the DMP chain transfer agent with cysteamine (33 mg, 9.15×10^{-5} mol) and followed the same reaction protocol except for increasing the reaction time to 48 h.

2.3. Synthesis of poly(ethyl acrylic acid-co-butyl methacrylate)-b-N-acryloxy succinimide copolymers

The first block of this diblock copolymer, poly(EAA-*co*-BMA) polymer, was dissolved in dioxane and mixed with *N*-acryloxy succinimide (NASI) monomers at a 1:56 M ratio in a round bottom Schlenk tube followed by purging with nitrogen for

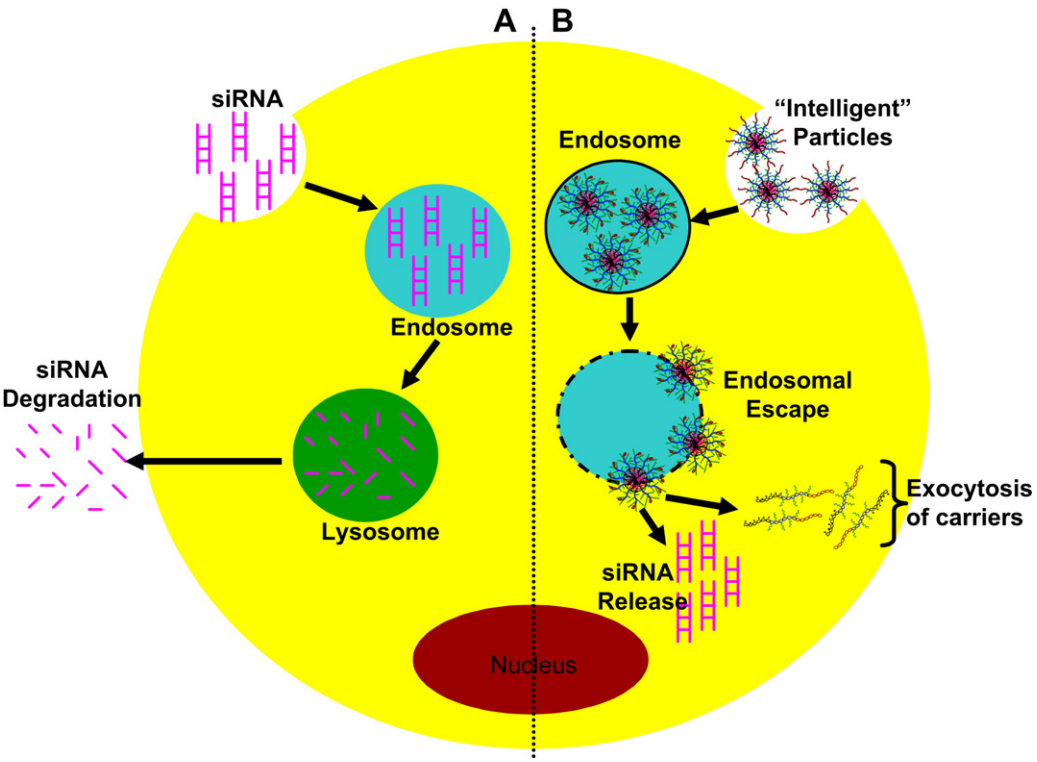

Fig. 1. A schematic drawing comparing the cellular fate of: (A) free nucleic acid molecules (e.g. siRNA) and (B) "intelligent" particles encapsulating therapeutic siRNA molecules. (A) Free siRNA molecules are internalized by endocytosis and get trapped in the endosomal-lysosomal trafficking pathway, which results in their degradation and loss of therapeutic activity. (B) Similarly, "intelligent" particles are internalized by endocytosis. In the endosome, the acid-labile hydrazone linkages connecting the comb-like grafts to the polymer backbone will be hydrolyzed in response to endosomal acidity. In addition, the pH-sensitive polymer backbone switches from a hydrophilic stealth-like conformation to a hydrophobic membrane-destabilizing one. The hydrophobic backbone and the polymer fragments synergistically rupture the endosomal membrane and release the encapsulated siRNA molecules into the cytoplasm to interact with their intracellular targets and produce the desired therapeutic activity. The polymer backbone and the fragmented grafts will be exocytosed and excreted in urine after delivering their cargo.

15 min. The AIBN initiator (5 mg, 3.0×10^{-5} mol) was added to the reaction mixture before placing the tube in an oil bath at 65 °C for 24 h (Fig. 4B). The crude polymer was dissolved in DMF, precipitated in diethyl ether, and dried under vacuum to yield pure poly(EAA-*co*-BMA)-b-NASI copolymer.

2.4. Synthesis of poly(ethyl acrylic acid-co-alkyl methyl acrylate)-b-β-benzyl L-aspartate copolymers

We dissolved poly(EAA-*co*-BMA)-NH_2 or poly(EAA-*co*-HMA)-NH_2 polymers synthesized by free radical polymerization in presence of cysteamine in DMF and mixed with β-benzyl L-aspartate *N*-carboxy-anhydride (BLA-NCA) monomers at a 1:100 M ratio in a round bottom Schlenk tube that was allowed to react at 50 °C for 48 h (Fig. 5B). BLA-NCA monomers reacted with the terminal NH_2 group of the first block through a ring-opening polymerization reaction forming the second poly(β-benzyl L-aspartate) block. The crude product was dissolved in DMF, precipitated in diethyl ether, and dried under vacuum to yield pure poly(EAA-*co*-BMA)-b-BLA and poly(EAA-*co*-HMA)-b-BLA polymers.

2.5. Graft polymerization of HMA and TMAEMA monomers via hydrazone linkages

The diblock polymer backbone with NASI and BLA blocks was used to synthesize macroinitiators for graft polymerization of HMA and TMAEMA monomers (Figs. 4C and 5C). The polymer backbone was dissolved in dimethyl sulfoxide (DMSO), mixed with anhydrous hydrazine in a Schlenk tube, and allowed to react at 40 °C for 24 h. The crude product was dissolved in DMF, precipitated in diethyl ether, and dried under vacuum to yield pure polymer-hydrazine conjugates, which was dissolved in DMSO and allowed to react with bromomalonaldehyde at a hydrazine-to-bromomalonaldehyde molar ratio of 1:1.5 for 24 h at room temperature. The pure macroinitiator was precipitated in acetone, filtered, and dried overnight under vacuum. The selected macroinitiator was dissolved in DMF, mixed with equimolar concentrations of HMA and TMAEMA monomers, the [Cu(I)Br] catalyst, and HMTETA ligand at a 1:1 M ratio followed by three freeze-vacuum-thaw cycles before placing the reaction mixture in an oil bath at 60 °C for 48 h while stirring. The molar ratio of the macroinitiator, HMA, and TMAEMA were controlled to prepare poly(HMA-*co*-TMAEMA) grafts with a weight average molecular weight (M_W) of 20 kDa equally split between the HMA and TMAEMA units. The final comb-like polymers were precipitated in diethyl ether, dried under vacuum, and further purified by dialysis against a NaOH solution (pH = 10) for 24 h followed by lyophilization for 48 h.

2.6. Characterization of the diblock backbone and comb-like grafts

The purity and composition of all the synthesized polymers were evaluated based on their ^{1}H NMR spectra in DMSO-d_6 recorded using a 300 MHz Varian Mercury system (Palo Alto, CA) at ambient temperature. The weight average molecular weight and molecular weight distribution of each polymer were examined based on their elution volume on an Ultrahydrogel 500 column compared to a series of poly(ethylene glycol) standards (Polymer Laboratories Ltd, UK) using Tris–HCL buffer (pH = 8) as a mobile phase at a flow rate of 0.5 ml/min. Detection of the eluting polymers was done using a Waters 2414 refractive index detector under the control of Breeze software run by an external PC (Waters Corporation, Milford, MA). Fragmentation of comb-like polymers in response to acidic environment was evaluated by dissolving 5 mg of each of the comb-like polymers in phosphate-buffered saline (PBS) with pH 5.8 and incubating at 37 °C for 24 h while stirring. A 100 μl sample was drawn from each of these polymer solutions at 0.5, 1, 2, 6, 12, and 24 h for analysis by gel permeation chromatography. The areas under the curve for the peaks corresponding to the parent comb-like polymer and poly(HMA-*co*-TMAEMA) fragments were used to quantify the amount of each polymer species present in solution at a given time point to determine the hydrolysis rate of the hydrazone linkages connecting the polymer grafts to the backbone.

2.7. Evaluation of the pH-dependent membrane-destabilizing activity of comb-like polymers

The membrane-destabilizing activity of the polymer backbone and comb-like polymers was assessed based on their ability to hemolyze red blood cells (RBCs) at different pH values. Briefly, human blood was collected in EDTA-containing vacutainers, which were centrifuged at 13,500 × g to separate the RBCs. The plasma supernatant was discarded and the RBCs were washed three times using a 150 mM saline solution. After the third wash, the RBCs solution was equally divided into three vacutainers and suspended in 100 mM PBS solutions with pH 5.8, 6.6, or 7.4.

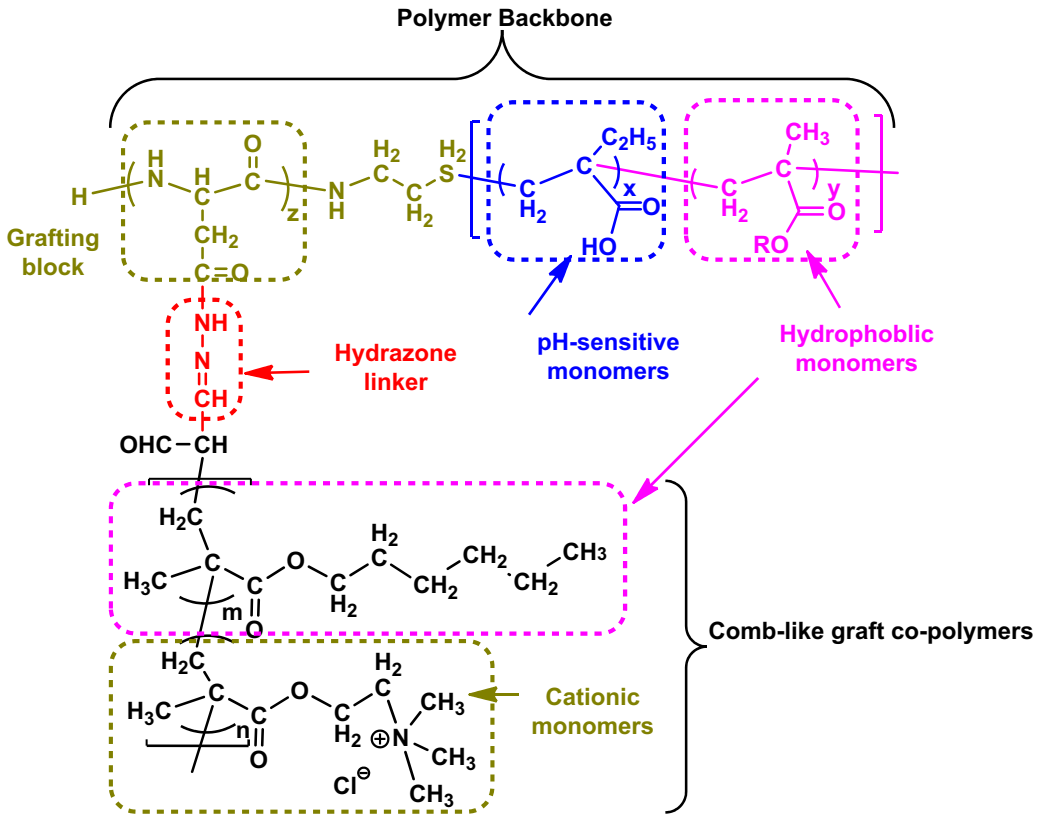

Fig. 2. A schematic drawing showing the chemical structure of a degradable, pH-sensitive, membrane-destabilizing, comb-like polymer. The first block in the diblock polymer backbone incorporates pH-sensitive (e.g. EAA) and hydrophobic (e.g. BMA and HMA) monomers. The second block incorporates *N*-acryloxy succinimide (NASI) or *ß*-benzyl L-aspartate *N*-carboxy-anhydride (BLA-NCA) monomers, which are functionalized to allow controlled grafting of hydrophobic HMA and cationic TMAEMA monomers via acid-labile hydrazone linkages.

The RBCs solutions were diluted 10-fold using PBS with the corresponding pH value to reach a concentration of 10^8 RBCs per 200 μl solution. Stock polymer solutions were prepared by dissolving each polymer in PBS solution of pH 7.4. The hemolytic activity of poly(EAA-*co*-BMA) and poly(EAA-*co*-HMA) copolymers and the comb-like polymers was evaluated as a function of polymer concentration (50, 100, and 200 μg/ml). The appropriate volume of the polymer stock solution was added to 800 μl of PBS solution and 200 μl of RBCs solution with the appropriate pH to reach the desired polymer concentration. The RBCs solutions were gently inverted several times for mixing with the added polymer solution then incubated for 60 min at 37 °C. The membrane-destabilizing activity of a given polymer was measured in terms of its ability to rupture the cell membrane of RBCs allowing the release of hemoglobin into the solution. At the end of the incubation time, RBCs solutions were centrifuged at 13,500 × g for 5 min to pellet out intact and ruptured RBCs leaving the hemoglobin in the supernatant solution. Absorbance of hemoglobin in the supernatant was measured at its characteristic wavelength, 541 nm. The observed hemolysis of RBCs in PBS solutions with different pH values and in DI water was used as negative and positive controls, respectively. The observed hemolytic activity of a given polymer at a given concentration and pH value was normalized to that of the positive control, DI Water. All hemolysis experiments were carried out in triplicate.

2.8. Formulation and characterization of "smart" particles

The pH-sensitive comb-like polymers were dissolved in RNase-free water and mixed with 0.5 μg of anti-GAPDH siRNA molecules dissolved in 1 μl of RNase free water at different nitrogen/phosphate (N/P) ratios. Each mixture was vortexed and allowed to stand at room temperature for 20 min before loading onto a 1% w/v agarose gel. The gel was immersed in a Tris-acetate-EDTA (TAE) buffer and run at 60 V for 1 h before staining with SYBR Green II dye (Pierce, Rockford, IL) for 30 min and visualized under UV using a fluorescent green filter (Fotodyne Incorporated, Hartland, WI). Size and zeta potential of the particles prepared using different comb-like polymers at N/P ratio of 2.5/1 were measured using 90Plus particle size analyzer with ZetaPALS capability (Brookhaven Instruments Corporation, Holtsville, NY).

2.9. Culture of MCF-7 cells

MCF-7 breast cancer cells were purchased from ATCC (Manassas, VA) and cultured following established protocols. Briefly, MCF-7 cells were maintained in Eagle's minimum essential medium (EMEM) supplemented with 10% fetal bovine serum, 0.01 mg/ml bovine insulin, 10,000 units/ml penicillin, 10,000 μg/ml streptomycin and regularly changing the growth medium every 2 days. MCF-7 cells were incubated at 37 °C, 5% CO_2, 95% relative humidity, and passaged upon reaching 70–90% confluency using 0.25% trypsin/EDTA mixture.

2.10. Cellular uptake of "smart" particles

Comb-like polymers and commercial siPORT-NH_2 were dissolved in OPTI-MEM solution and mixed with 0.57 μg of FAM-labeled anti-GAPDH siRNA molecules at N/P ratios of 1.5/1, 2.5/1, 4/1, 8/1, and 12/1 to prepare different particles that were incubated with MCF-7 cells for 6 h at 37 °C, 5% CO_2, and 95% relative humidity. MCF-7 cells were washed with PBS, treated with 0.25% trypsin/EDTA solution for 10 min, harvested, and centrifuged to remove the supernatant and form a cell pellet. MCF-7 cell pellets were suspended in PBS and analyzed using Biosciences FACSCalibur (Becton Dickinson, Franklin Lakes, NJ) to determine the percentage of fluorescently-labeled MCF-7 cells for each treatment. MCF-7 cells were gated by forward/size scatter and 10,000 gated events were collected per sample to discriminate between live and dead cells and account for live cells only.

2.11. In vitro transfection of MCF-7 cells

MCF-7 cells were plated in 24-well plates at a seeding density of 40,000 cells/well and allowed to adhere for 24 h. The particles and siPORT-NH_2 complexes incorporating 0.57 μg of anti-GAPDH siRNA or control siRNA molecules were incubated with MCF-7 cells at a final siRNA concentration of 100 nM for 6 h followed by addition of 500 μl of fresh culture medium and incubation for a total of 48 h. The effect of different treatments on GAPDH expression was quantified based on mRNA and protein levels. For quantification of mRNA, total RNA was isolated from MCF-7 cells using the RNeasy Mini Kit and 0.25 μg of total RNA was reverse transcribed using Omniscript reverse transcriptase kit following manufacturer's protocols. Real-time PCR was performed in a final volume of 20 μl containing 2 μl of cDNA (corresponding to 10 ng of total RNA for GAPDH and β-actin amplification), 1 μl of each primer, and 10 μl of the qPCR Master Mix in the 7500 Fast Real-Time PCR system. The amount of GAPDH protein expressed by MCF-7 cells was measured using the kDalert assay following manufacturer's specifications. The

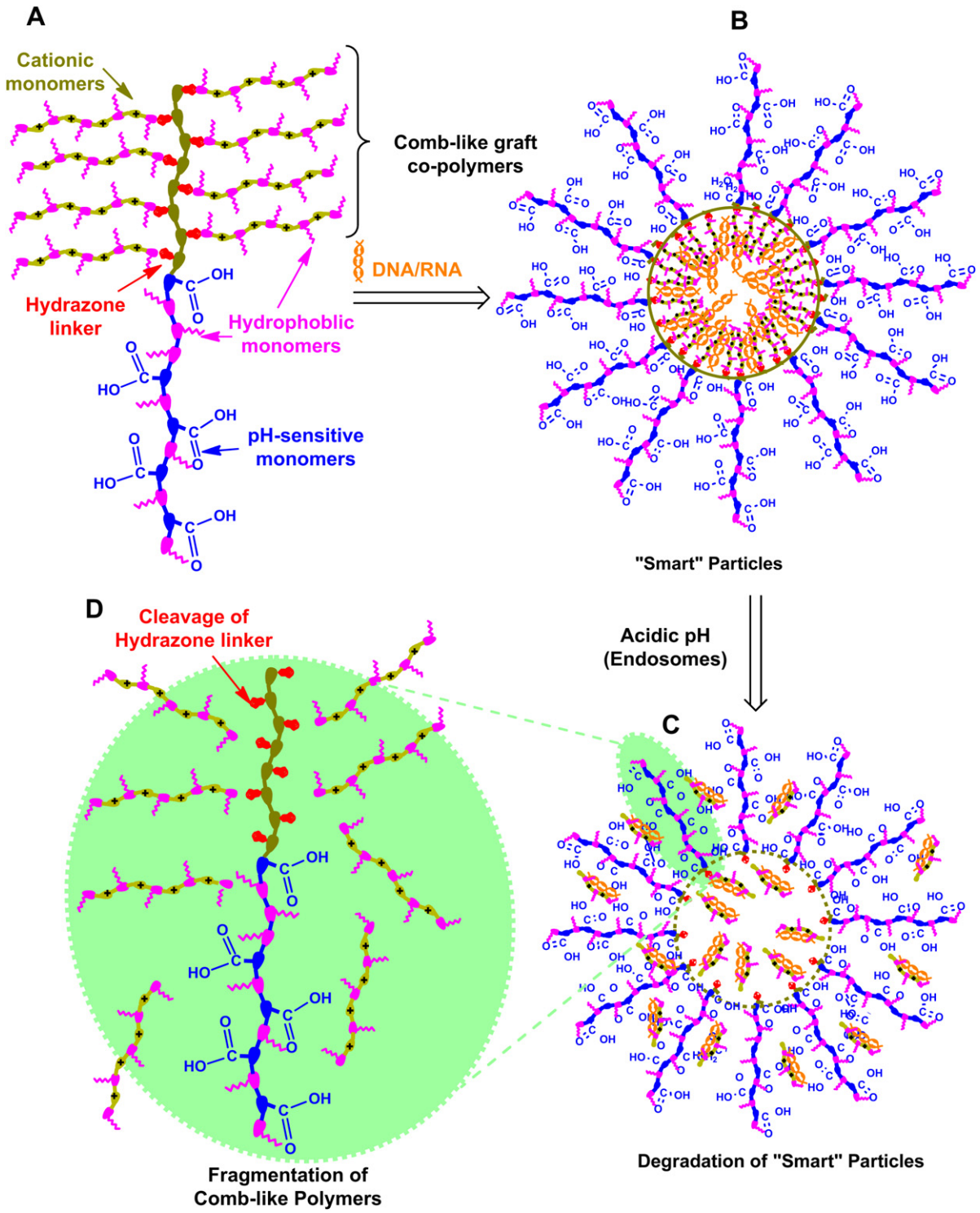

Fig. 3. A schematic drawing showing the structure of a comb-like polymer, complexation of siRNA molecules into "smart" particles, their response to acidic pH, and fragmentation of the comb-like carrier. (A) is a schematic of a degradable, pH-sensitive, membrane-destabilizing, comb-like polymer at pH 7.4 with intact hydrazone linkages between the grafts and the polymer backbone. (B) This polymer condenses therapeutic nucleic acids into "smart" particles, which remain intact at neutral pH but degrade upon exposure to acidic endosomal pH gradients (C) due to hydrolysis of the acid-labile hydrazone linkage and fragmentation of the comb-like carrier (D).

level of GAPDH protein expression in response to different treatments was normalized to that of untreated control cells.

2.12. *Effect of serum and nuclease enzymes on stability of "smart" particles*

The particles were prepared by mixing pH-sensitive comb-like polymers with 0.57 μg of anti-GAPDH siRNA molecules at a N/P (+/−) ratio of 2.5/1 followed by addition of 10 or 25% FBS and incubation at 37 °C for 6 h. The amount of siRNA released from different particles was measured by adding the PicoGreen dye and measuring the fluorescence intensity using a Fluoroskan microplate reader (Thermo Fisher Scientific Inc., Waltham, MA) at λ_{ex} of 485 nm and λ_{em} of 518 nm. The fluorescence intensity of each solution was normalized to that observed upon mixing the PicoGreen dye with 0.57 μg of anti-GAPDH siRNA to determine the amount of free siRNA present in solution.

The enzymatic stability of particle 1 was assayed using the gel retardation assay. Briefly, poly(EAA-*co*-BMA)-b-NASI-g-(HMA-*co*-TMAEMA) comb-like

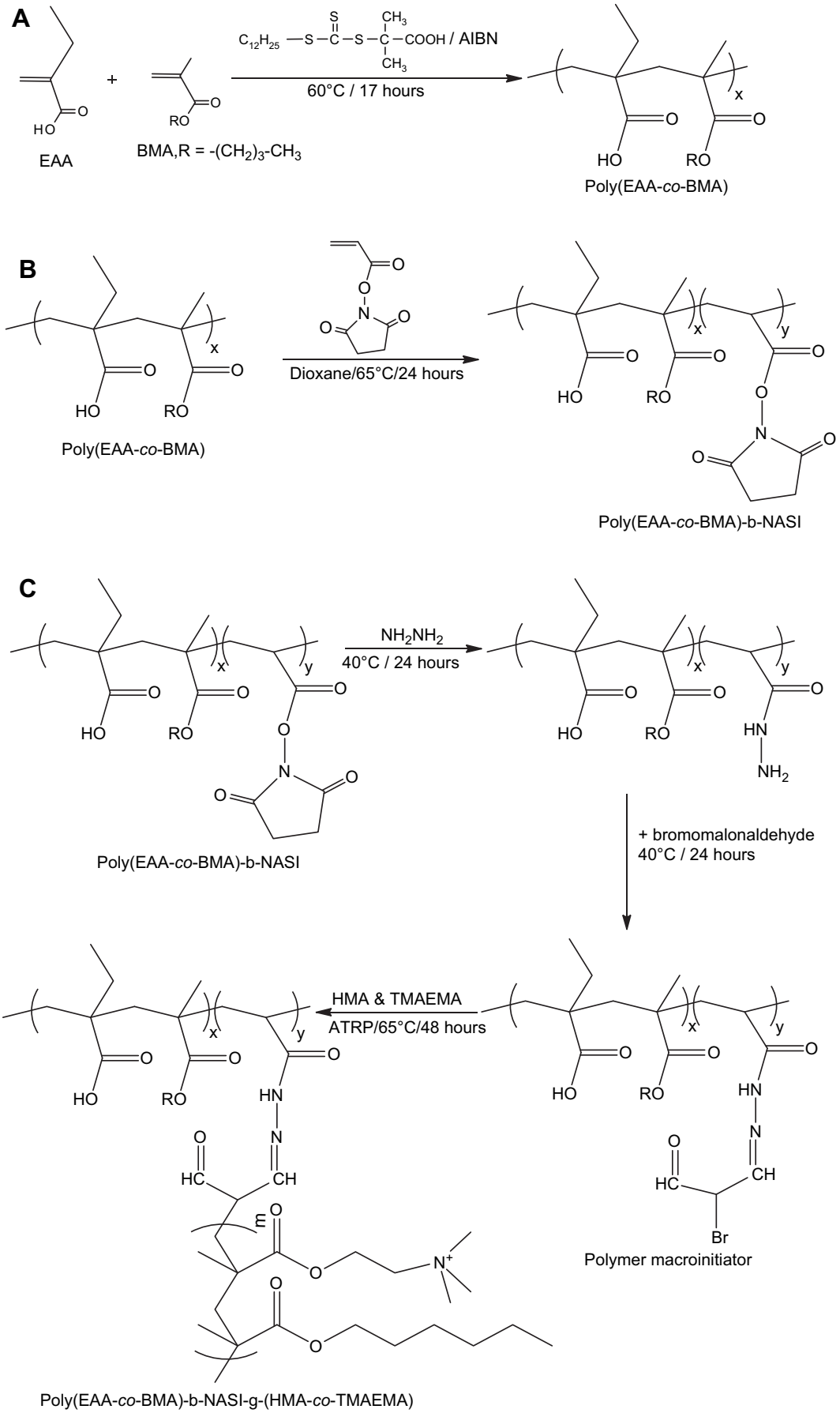

Fig. 4. Protocol for synthesis of poly(EAA-*co*-BMA)-b-NASI-g-(HMA-*co*-TMAEMA) comb-like polymer.

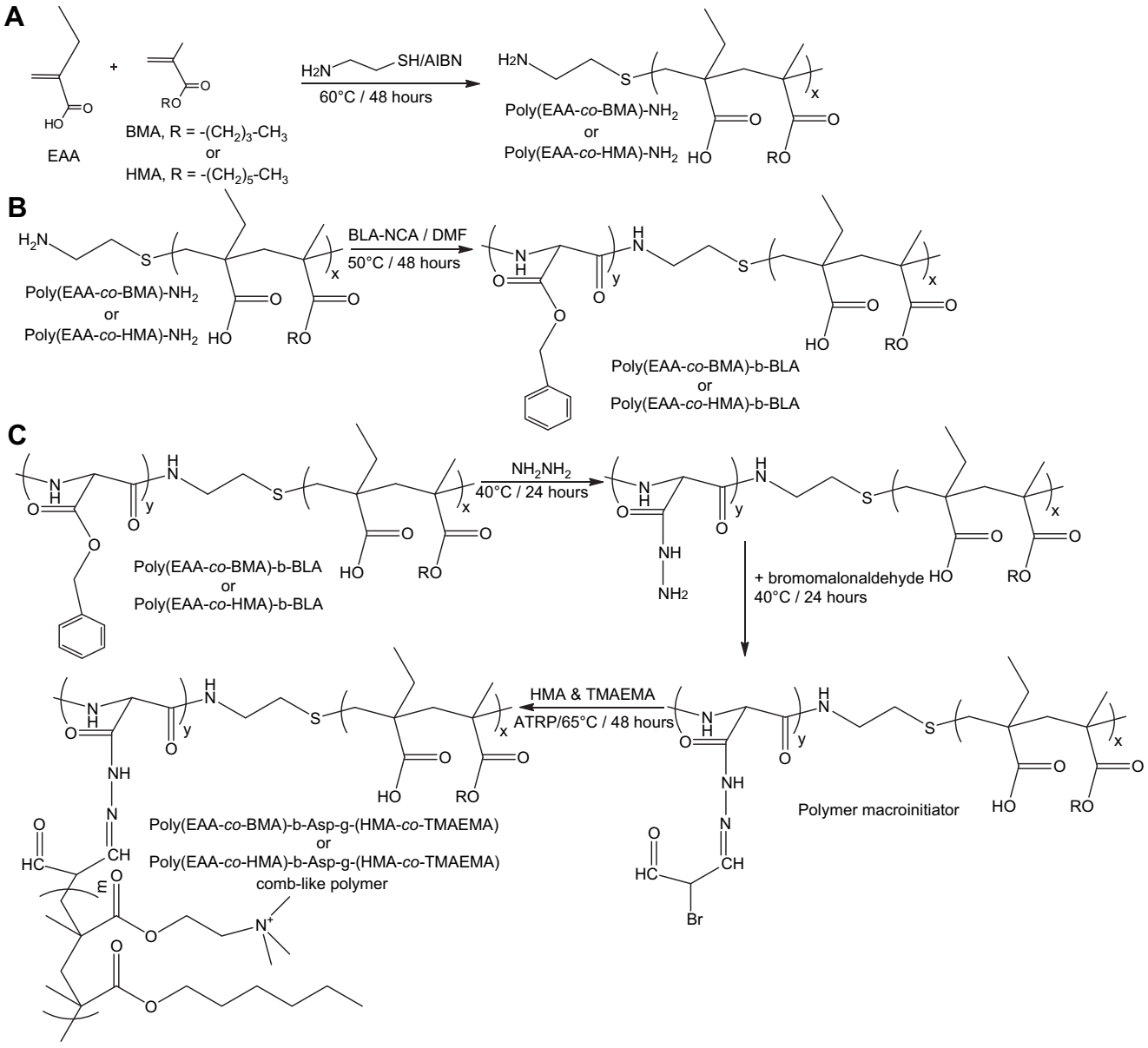

Fig. 5. Protocol for synthesis of poly(EAA-*co*-BMA)-b-Asp-g-(HMA-*co*-TMAEMA) and poly(EAA-*co*-HMA)-b-Asp-g-(HMA-*co*-TMAEMA) comb-like polymers.

polymer was dissolved in RNase-free water and mixed with 0.57 μg of anti-GAPDH siRNA molecules at N/P (+/−) ratios of 1/1, 2.5/1, 4/1, 8/1, and 12/1. Free siRNA and the complexes prepared at different N/P ratios were incubated with RNase V1 enzyme at 37 °C for 30 min before loading onto a 1% w/v agarose gel, which was subjected to 60 mV electric current for 60 min and stained with SYBR Green II dye. UV was used to visualize siRNA shift. The fluorescence intensity of each band for the complexes treated with the RNase enzyme (+) was compared to that of complexes not treated (−) with the RNase enzyme using free siRNA as a control.

3. Results and discussion

3.1. Synthesis of degradable, pH-sensitive, membrane-destabilizing, comb-like polymers

The focus of this work is the design and synthesis of pH-sensitive carriers that can successfully condense a large dose of DNA/RNA molecules into particles that will be internalized into target cells via endocytosis. In the endosome, these particles will "sense" the drop in pH, which triggers their degradation into small membrane-destabilizing fragments that disrupt the endosomal membrane and release the encapsulated nucleic acid into the cytoplasm to interact with specific intracellular targets to produce the desired therapeutic activity (Fig. 3). These degradable, pH-sensitive, membrane-destabilizing, comb-like polymers are constructed on a diblock polymer backbone where the first block incorporates pH-sensitive EAA and hydrophobic BMA or HMA monomers at a 60/40 M feed ratio. The second block in the backbone is either *N*-acryloxy succinimide (NASI) or ß-benzyl L-aspartate *N*-carboxy-anhydride (BLA-NCA) monomers to allow controlled grafting of poly(HMA-*co*-TMAEMA) copolymers via acid-labile hydrazone linkages.

Results show that the first block in the polymer backbone, poly (EAA-*co*-BMA) and poly(EAA-*co*-HMA) copolymers, was successfully synthesized by RAFT and random free radical polymerization techniques with average yields of 97.2% and 91.7%, respectively. The molar ratio of EAA to BMA/HMA monomers in the synthesized polymers is approximately 55/45, which is similar to their feed ratio (Table 1). Controlled addition of the NASI monomers to poly

(EAA-*co*-BMA) polymer yielded a diblock copolymer with an average polymerization yield of 90%. Similarly, poly(EAA-*co*-BMA)-NH_2 and poly(EAA-*co*-HMA)-NH_2 polymers reacted with BLA-NCA monomers via a ring-opening polymerization reaction to yield a diblock copolymer with an average yield of 92%. Both NASI- and BLA-containing polymers reacted with hydrazine and bromomalonoaldehyde to yield macroinitiators that incorporate an acid-labile hydrazone linkage. Atom transfer radical polymerization (ATRP)-controlled grafting of HMA and TMAEMA monomers to poly(EAA-*co*-BMA)-b-NASI backbone was efficient and produced 22 comb-like grafts, which account for 93% of the Br-activated NASI monomers present in the polymer backbone (Table 1). The molar ratio of HMA to TMAEMA monomers in the grafts closely followed their feed ratio (Table 1). Grafting of HMA and TMAEMA monomers to poly(EAA-*co*-BMA)-b-BLA and poly(EAA-*co*-HMA)-b-BLA polymers yielded 4 and 10 comb-like grafts, which account for grafting efficiencies of 37% and 38%, respectively (Table 1). It is important to note that NASI-containing polymers have a higher positive charge density compared to BLA-containing polymers due to the higher number of grafts attached per polymer backbone where poly(EAA-*co*-BMA)-b-NASI-g-(HMA-*co*-TMAEMA) comb-like polymer has the highest TMAEMA content per unit weight. The variation in TMAEMA content will vary the amount of comb-like polymer necessary to complex a given dose of nucleic acid producing particles with different polymer content.

The pH-responsiveness of these comb-like polymers is in part a result of using hydrazone linkages to connect the poly(HMA-*co*-TMAEMA) grafts to the polymer backbone. Hydrazone linkages have previously been used to conjugate small molecular weight anticancer drugs (e.g. doxorubicin) to water-soluble HPMA polymers and proved to hydrolyze and release the attached drug upon internalization into acidic intracellular vesicles [42–48]. Torchilin and coworkers conjugated PEG chains to TAT-modified liposomes via hydrazone linkers to shield the liposomes from the reticular endothelial system, increase their plasma residence time, and enhance their accumulation into tumor and ischemic tissues. The hydrazone linkage connecting the PEG chains to the lipid shell is hydrolyzed in the acidic environment of tumor and ischemic tissues, which unmasks the TAT peptide and trigger cell uptake [49–52]. Hydrazone linkages have also been used to allow controlled degradation of temperature-sensitive hydrogels used for site-specific delivery of radioactive nuclides [53].

The motivation to incorporate acid-labile hydrazone linkages in these comb-like polymers is to allow the grafting of a large number of cationic/hydrophobic polymer chains onto the polymer backbone to achieve a high positive charge density that will allow the condensation of a large number of DNA/RNA molecules into pH-sensitive particles with high therapeutic loading. The molecular weight of a cationic non-degradable polymer that can condense a similar dose of nucleic acids would exceed 250 kDa, which would result in non-specific cellular toxicity due to its poor degradation and elimination. On the other hand, the hydrzone linkages connecting poly(HMA-*co*-TMAEMA) grafts to the polymer backbone will hydrolyze in response to the acidity of the endosome, which will result in fragmenting the comb-like polymeric carrier into the backbone and multiple grafts with average molecular weights of 40–45 and 20 kDa, respectively. These smaller fragments are hydrophilic and can be easily eliminated *in vivo* by renal excretion, which will significantly diminish their toxicity. Our results show that poly(EAA-*co*-BMA)-b-NASI-g-(HMA-*co*-TMAEMA), poly(EAA-*co*-BMA)-b-Asp-g-(HMA-*co*-TMAEMA), and poly(EAA-*co*-HMA)-b-Asp-g-(HMA-*co*-TMAEMA) comb-like polymers have similar degradation profiles with degradation half lives ($t_{1/2}$) of 1.0, 1.2, and 0.75 h, respectively (Fig. 6). Earlier research showed that acidification of endocytic vesicles loaded with cationic particles occurs within 15 min with drop in environment pH to 5.9 [54], which suggests that degradation of the particles prepared using these comb-like polymers will start shortly after their internalization and result in a rapid escape of the nucleic acid cargo into the cytoplasm. These comb-like polymers exhibited insignificant (<5%) degradation at pH 7.4, which indicates that their membrane-destabilizing activity will be limited to the endosomal compartment, which enhances their overall biocompatibility.

3.2. Membrane-destabilizing activity of comb-like polymers

The membrane-destabilizing activity of the polymer backbone and comb-like polymers was assessed based on their hemolytic activity as a function of polymer concentrations (50, 100, and 200 μg/ml) and solution pH (pH 5.8, 6.6, and 7.4). This hemolysis

Table 1
Composition of new degradable, pH-sensitive, membrane-destabilizing, comb-like polymers.

Polymer Name	Molecular Weight (g/mol)[a]	Monomers Molar Ratio[b]	Number of NASI or BLA Monomers[d]	Number of Grafts/ Grafting Efficiency[e]	Number of TMAEMA Units per Graft/ Comb-like Polymer[f]	Number of HMA Units per Graft/Comb-like Polymer[g]
Poly(EAA-*co*-BMA)	33,000	54.9:45.1	–	–	–	–
Poly(EAA-*co*-BMA)-b-NASI	37,000	51.3:36.2:12.5	24	–	–	–
Poly(EAA-*co*-BMA)-b-NASI-g-(HMA-*co*-TMAEMA)	481,000	48.3:51.7[c]	24	22/93	60/1330	57/1250
Poly(EAA-*co*-BMA)-NH_2	56,000	59.05:40.95	–	–	–	–
Poly(EAA-*co*-BMA)-b-BLA	58,000	54.6:29.2:16.1	11	–	–	–
Poly(EAA-*co*-BMA)-b-Asp-g-(HMA-*co*-TMAEMA)	135,000	54.5:45.5[c]	11	4/37	53/205	64/247
Poly(EAA-*co*-HMA)-NH_2	52,000	59.1:40.9	–	–	–	–
Poly(EAA-*co*-HMA)-b-BLA	57,000	40.9:41.6:17.4	26	–	–	–
Poly(EAA-*co*-HMA)-b-Asp-g-(HMA-*co*-TMAEMA)	256,000	41.2:58.8[c]	26	10/38	69/684	49/482

[a] The weight average molecular weight of each polymer is calculated based on its retention volume in relation to the elution volumes of a series of poly(ethylene glycol) standards run on an Ultrahydrogel 500 column using Tris-HCL buffer (pH = 8) as a mobile phase at a flow rate of 0.5 ml/min.
[b] Monomer's molar ratio determined using the ^{1}H NMR spectra of the pure polymer.
[c] The molar ratio of the HMA and TMAEMA monomers incorporated in the comb-like grafts determined using the ^{1}H NMR spectra of the pure polymer.
[d] The number of NASI and BLA monomers incorporated in the second block of the polymer backbone calculated using the ^{1}H NMR spectra of the pure polymer.
[e] The number of poly(HMA-*co*-TMAEMA) grafts attached to the polymer backbone calculated based on the molecular weight of the comb-like polymer. Grafting efficiency is based on the ratio between the number of grafts to the number of NASI or BLA monomers incorporated in the polymer backbone.
[f] The number of cationic TMAEMA monomers is calculated based on its molar content in the grafts. The total number of TMAEMA monomers in the comb-like polymer accounts for the total number of the grafts.
[g] The number of hydrophobic HMA monomers is calculated based on its molar content in the grafts. The total number of HMA monomers in the comb-like polymer accounts for the total number of the grafts.

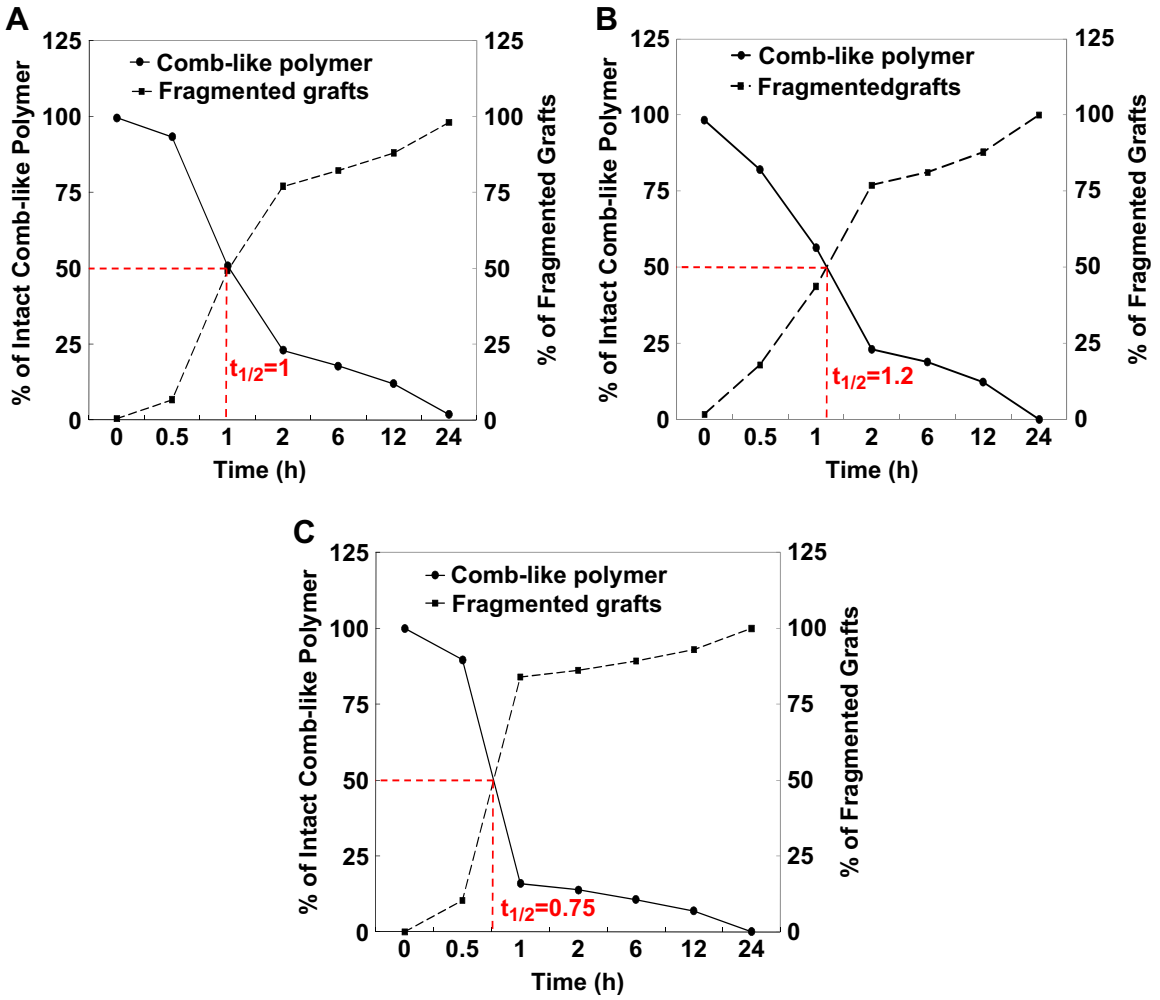

Fig. 6. A plot correlating the change in the areas under the curve for the amount of parent (A) poly(EAA-*co*-BMA)-b-NASI-g-(HMA-*co*-TMAEMA), (B) poly(EAA-*co*-BMA)-b-Asp-g-(HMA-*co*-TMAEMA), and (C) poly(EAA-*co*-HMA)-b-Asp-g-(HMA-*co*-TMAEMA) comb-like polymers and the released poly(HMA-*co*-TMAEMA) fragments upon incubation of these polymers in phosphate-buffered saline solutions with pH 5.8 at 37 °C for 24 h. The areas under the curve of the peaks corresponding to the parent comb-like polymer (●) and the fragmented poly(HMA-*co*-TMAEMA) grafts (■) on an Ultrahydrogel 500 column were used to calculate the % of the intact comb-like polymer and the released fragments upon hydrolysis of the hydrazone linkages in this acidic medium as a function of the incubation time.

assay is based on the established correlation between the observed hemolytic activity at acidic pH values and endosomal membrane disruption [25,55,56]. Polymers that exhibited a hemolytic activity ≥50% of that observed with the positive control (DI water) at acidic pH values has the potential to function as endosomolytic carriers. The hemolytic activity of poly(EAA-co-BMA) and poly(EAA-co-HMA) copolymers prepared by random free radical and RAFT polymerization techniques caused ≥75% hemolysis of the red blood cells at all concentrations and pH values (Fig. 7). This high hemolytic activity at all pH values is attributed to high BMA and HMA (45%) and low EAA (55%) content, which reduces the ability of these copolymers to sense the changes in environment pH compared to polymers with higher (>75%) acrylic acid content [37,38]. Earlier results clearly showed that conjugation of cationic peptides and complexation with nucleic acids shift the polymer's hydrophilic/hydrophobic balance towards being more hydrophilic, which tunes its pH-responsiveness but can possibly reduce its membrane-destabilizing activity [38]. We hypothesized that these highly hemolytic polymers will retain their membrane-destabilizing activity upon grafting of cationic TMAEMA monomers and complexation with nucleic acids. Consequently, we utilized these poly(EAA-*co*-BMA) and poly(EAA-*co*-HMA) copolymers as the primary block in the backbone of the synthesized comb-like polymers.

Grafting of cationic poly(TMAEMA) polymers onto the polymer backbone via acid-labile hydrazone linkages significantly reduced the hemolytic activity of these polymers, which prompted us to incorporate an equal molar concentration of hydrophobic HMA monomers in the graft composition to enhance the membrane-destabilizing activity of the final comb-like polymer (data not shown). The hemolytic activity of poly(EAA-*co*-BMA)-b-NASI-g-(HMA-*co*-TMAEMA) comb-like polymer was ≥90% at acidic pH values of 6.6 and 5.8 at each of the studied concentrations (Fig. 8A). At pH 7.4, the hemolytic activity of this polymer gradually increased from 60% to 88% with the increase in polymer concentration from 50 to 200 μg/ml, which can be a result of the high concentration of TMAEMA quaternary amine groups present in solution. Recent results showed that amphiphilic polymers incorporating quaternary amine groups cause pH-independent cell lysis [57]. Poly(EAA-*co*-BMA)-b-Asp-g-(HMA-*co*-TMAEMA) comb-like polymer exhibited a clear pH- and concentration-dependant hemolytic profile (Fig. 8B). At a concentration 50 μg/ml, the polymer produced a low hemolytic activity (29%) at pH 7.4 that increased to 54% and 45% at acidic pH of 6.6 and 5.8, respectively (Fig. 8B). The hemolytic

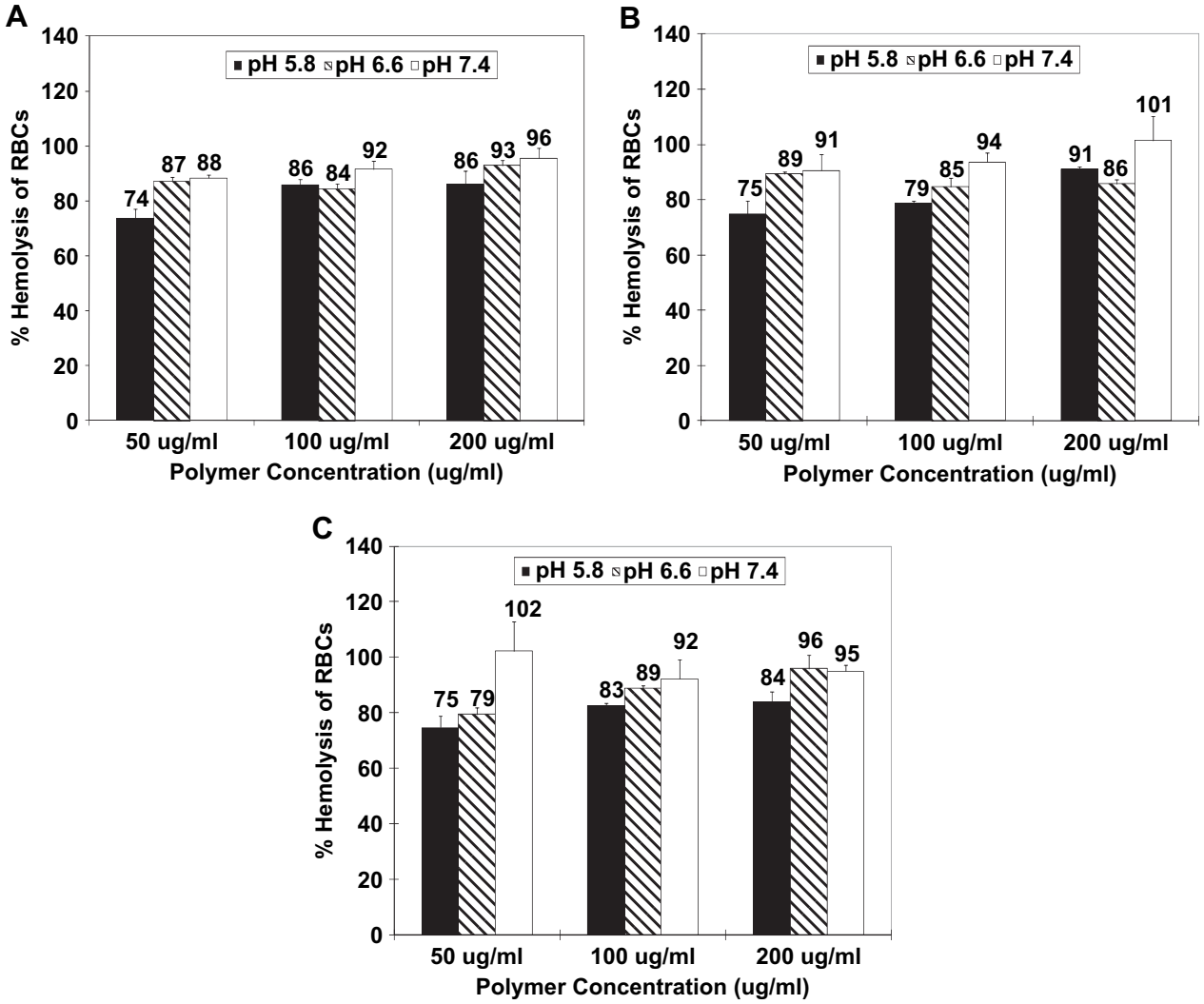

Fig. 7. The hemolytic activity of poly(EAA-*co*-BMA) (A & B) and poly(EAA-*co*-HMA) (C) copolymers synthesized by random free radical (A & C) and reversible addition-fragmentation chain transfer (RAFT) polymerization techniques (B). Hemolysis results are the average + the standard error of the mean of three independent experiments each carried out in triplicates. The observed hemolytic activity for each polymer is normalized to that of the positive control (DI water).

activity significantly increased with the increase in polymer's concentration reaching 80%–90% hemolysis at acidic pH values with a less pronounced increase at physiologic pH of 7.4 (Fig. 8B). Similarly, poly(EAA-*co*-HMA)-b-Asp-g-(HMA-*co*-TMAEMA) comb-like polymer showed a low hemolytic activity at pH 7.4 compared to that observed at acidic pHs of 6.6 and 5.8, which increased with the increase in polymer's concentration (Fig. 8C). The observed hemolytic activity of these polymers in acidic environment (pH 6.6 and 5.8) is attributed to the pH-sensitive poly(EAA-*co*-BMA) and poly(EAA-*co*-HMA) blocks in the polymer backbone aided with the hydrophobic HMA monomers embedded in the poly(HMA-*co*-TMAEMA) grafts, which get released into acidic solutions upon hydrolysis of the connecting hydrazone linkages. Hemolysis results indicate that all comb-like polymers exhibit a concentration-dependent membrane-destabilizing activity in response to acidic stimuli, which suggests their potential as carriers for intracellular delivery of therapeutic nucleic acids.

3.3. Formulation of "smart" particles

The ability of comb-like polymers to condense anti-GAPDH siRNA molecules into pH-sensitive particles was analysed using the standard gel retardation assay. Comb-like polymers were mixed with a fixed amount (0.5 μg) of anti-GAPDH siRNA molecules at different N/P (+/−) ratios where the electrostatic interaction between the cationic quaternary amine groups of the TMAEMA monomers and the anionic phosphate groups of the RNA molecules will lead to formation of particles that encapsulate the loaded RNA molecules. The amount of each comb-like polymer needed to complex the loaded siRNA molecules varied based on their TMAEMA content. Results show that all comb-like polymers successfully complexed the loaded siRNA molecules at all N/P ratios, which is indicated by their retention in the loading wells compared to the observed migration of free siRNA molecules (Fig. 9). It is important to note that poly(EAA-*co*-BMA)-b-Asp-g-(HMA-*co*-TMAEMA) and poly(EAA-*co*-HMA)-b-Asp-g-(HMA-*co*-TMAEMA) polymers fully condensed the loaded siRNA molecules at a 1/1 N/P ratio whereas poly(EAA-*co*-BMA)-b-NASI-g-(HMA-*co*-TMAEMA) polymer partially condensed the same amount of siRNA molecules at a 1/1 N/P ratio and fully condensed the loaded siRNA molecules at 2/1 N/P ratio (Fig. 9). This clearly shows that these new comb-like polymers can condense siRNA molecules at low N/P ratios compared to other acrylic acid-based polymers [37,38]. This reduces the amount of comb-like polymers needed to complex

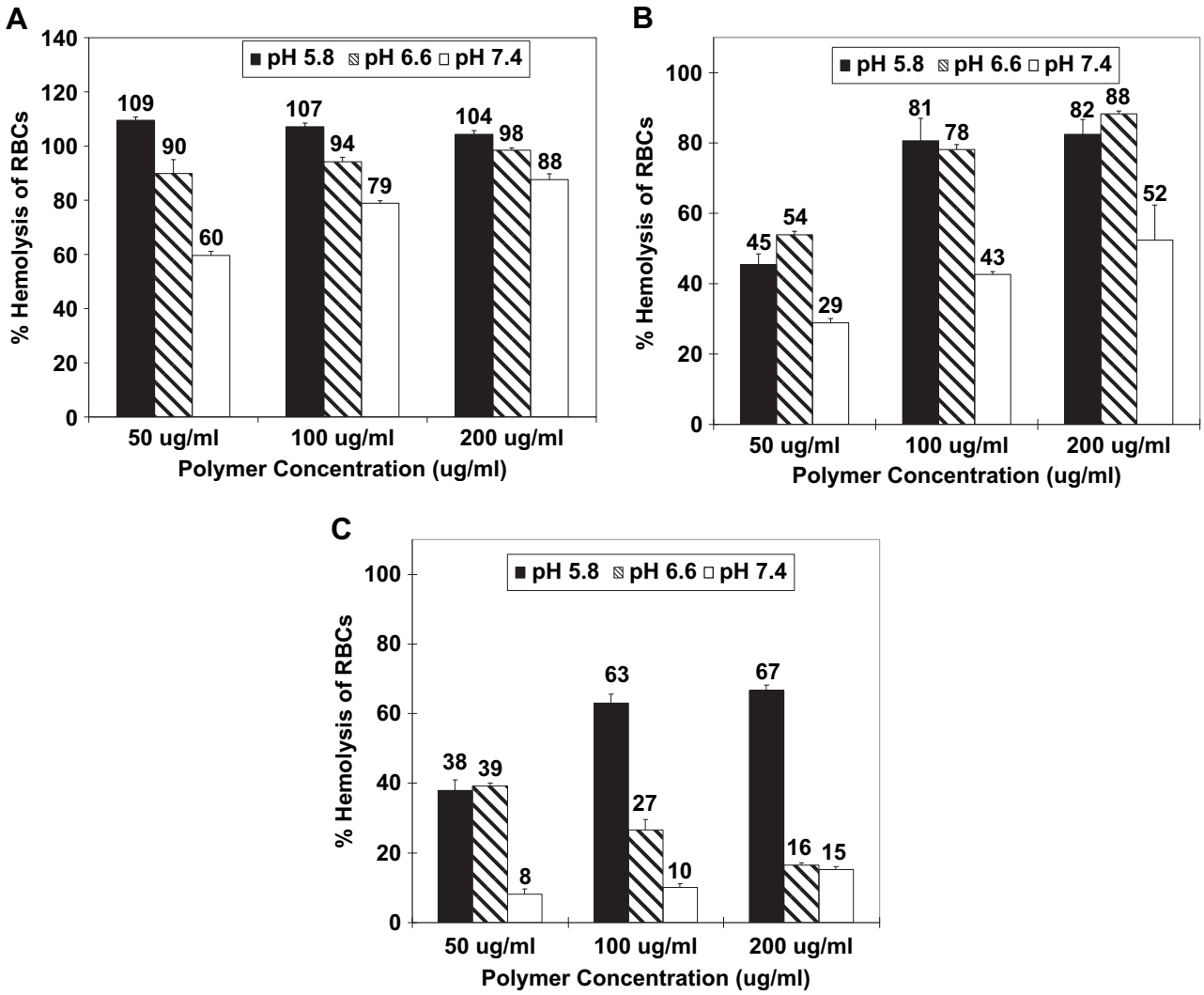

Fig. 8. Hemolytic activity of (A) poly(EAA-*co*-BMA)-b-NASI-g-(HMA-*co*-TMAEMA), (B) poly(EAA-*co*-BMA)-b-Asp-g-(HMA-*co*-TMAEMA) and (C) poly(EAA-*co*-HMA)-b-Asp-g-(HMA-*co*-TMAEMA) comb-like polymers as a function of polymer concentration and solution pH. Results are the average + the standard error of the mean of three independent experiments each carried out in triplicates. The observed hemolytic activity for each polymer is normalized to that of the positive control (DI water).

a given dose of therapeutic nucleic acids and consequently minimizes the toxicity commonly associated with cationic carriers.

3.4. Membrane-destabilizing activity of "smart" particles

Comb-like polymers have to retain their membrane-destabilizing activity after their complexation with nucleic acid molecules in order to disrupt the endosomal membrane and release their therapeutic cargo into the cytoplasm in response to the acidic endosomal pH gradients. Conjugation of cationic peptides and complexation with DNA molecules have been shown to reduce the membrane-destabilizing activity of other pH-sensitive polymers due to a shift in the hydrophilic/hydrophobic balance in the formed complexes towards being more hydrophilic [37,38]. Consequently, we evaluated the hemolytic activity of the particles prepared by complexation of comb-like polymers with 0.5 μg of anti-GAPDH siRNA molecules at N/P ratio of 2.5/1 as a function of solution pH. Results show that all particles exhibited a sharp membrane-destabilizing activity in acidic solutions (pH 5.8) compared to neutral ones (pH 7.4), which indicates their ability to "sense" the drop in environment pH (Fig. 10). At pH 5.8, the particles formulated based on NASI-containing polymer displayed a high hemolytic activity (84%) compared to Asp-containing polymers, which displayed a lower hemolytic activity in the range of 66%–72%. All particles except those prepared using Poly(EAA-*co*-BMA)-b-NASI-g-(HMA-*co*-TMAEMA) comb-like polymers showed a low hemolytic activity at pHs 6.6 and 7.4, which clearly indicates the tuning of the membrane-destabilizing activity of these comb-like carriers upon complexation with nucleic acid molecules. This hemolysis profile clearly shows the membrane-disruptive activity of these particles in response to acidic endosomal pH gradients, which suggests their potential as carriers for enhancing the cytoplasmic delivery of nucleic acids.

3.5. Characterization of "smart" particles

Size and surface charge of these particles were measured using dynamic light scattering and zeta potential measurements, respectively. Results show that particles 1 and 3 have similar particle size in the range of 400–430 nm compared to particles 2, which have a larger size of 666 nm (Fig. 11A). All particles display a cationic surface with an average zeta potential of 23–35 mV (Fig. 11B). The combination of size and surface charge dictates the ability of these particles to escape recognition and scavenging by

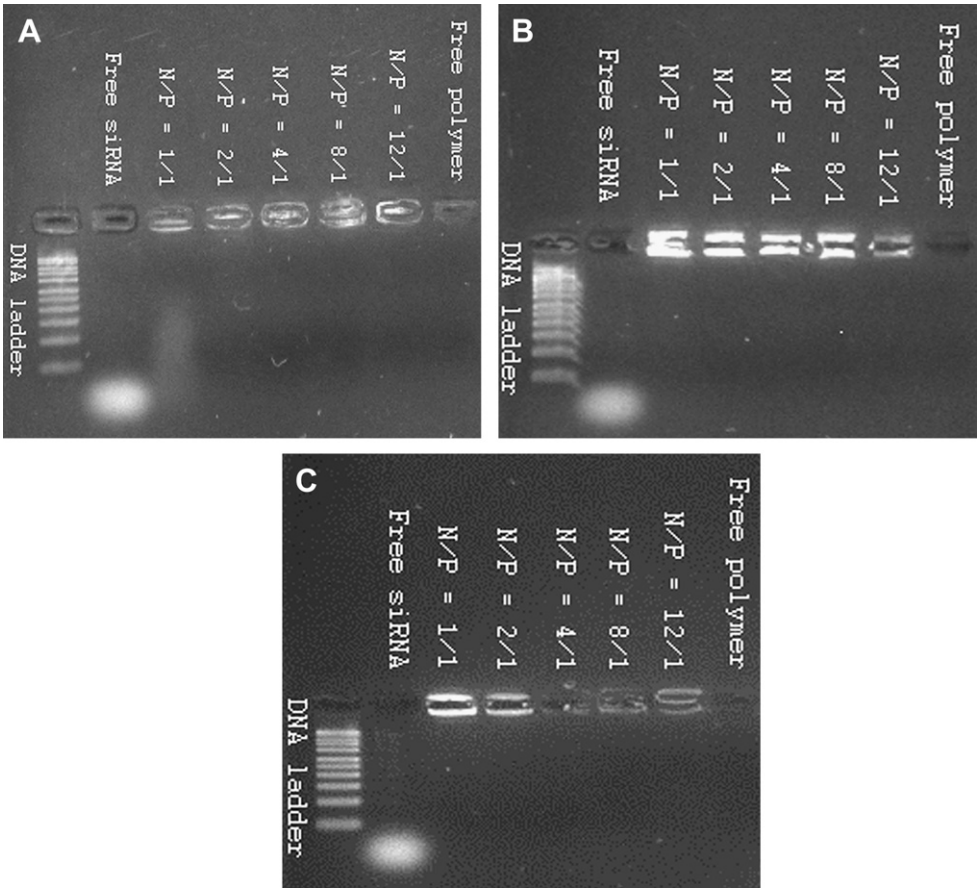

Fig. 9. Images of the 1% w/v agarose gels stained with SYBR Green II dye showing the electrophoretic mobility of free siRNA and the particles prepared by complexing (A) poly(EAA-*co*-BMA)-b-NASI-g-(HMA-*co*-TMAEMA), (B) poly(EAA-*co*-BMA)-b-Asp-g-(HMA-*co*-TMAEMA) and (C) poly(EAA-*co*-HMA)-b-Asp-g-(HMA-*co*-TMAEMA) comb-like polymers with 0.5 μg of anti-GAPDH siRNA molecules at different N/P (+/−) ratios.

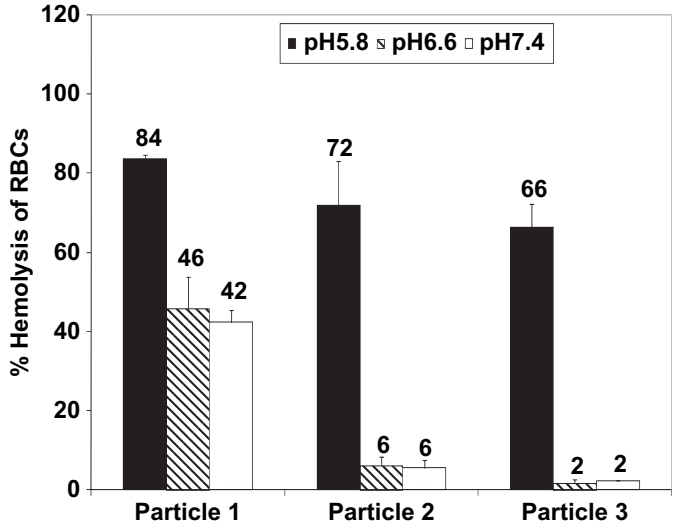

Fig. 10. The hemolytic activity of particles 1–3 prepared by complexing poly(EAA-*co*-BMA)-b-NASI-g-(HMA-*co*-TMAEMA), poly(EAA-*co*-BMA)-b-Asp-g-(HMA-*co*-TMAEMA), and poly(EAA-*co*-HMA)-b-Asp-g-(HMA-*co*-TMAEMA) comb-like polymers with 0.5 μg of anti-GAPDH siRNA molecules at a N/P ratio of 2.5/1. Results are the average + the standard error of the mean of three independent experiments each carried out in triplicates. The observed hemolytic activity is normalized to that of the positive control (DI water).

the reticular endothelial system, extravasate from the systemic circulation into tumor tissue, and become effectively internalized by target cells. Earlier research showed that the molecular size cut off for tumor vasculature is between 400 and 600 nm [58]. Consequently, these particles particularly 1 and 3 are suited for delivery of nucleic acids into solid tumors. Additionally, the cationic nature of these particles will facilitate their interaction and internalization into target cells via adsorptive endocytosis, which further emphasizes their potential as drug carriers.

3.6. Uptake of "smart" particles into MCF-7 breast cancer cells

We evaluated the internalization of fluorescently-labeled particles 1–3 prepared at different N/P ratios into MCF-7 breast cancer cells in comparison to complexes prepared using commercial siPORT amine transfection agent using flow cytometry. Results show that free siRNA molecules were not internalized and require a carrier to enhance their uptake by MCF-7 cancer cells (Fig. 12). At low N/P ratios of 1.5/1 and 2.5/1, particles 3 showed higher uptake into MCF-7 cells compared to particles 2, which exhibited higher uptake than particles 1. However, at higher N/P ratios, all particles exhibited a similar uptake profile into MCF-7 cells, which can be attributed to their higher positive charge density due to the incorporation of excess comb-like polymers into these particles. Similarly, siPORT amine-based complexes showed high internalization (95%) into MCF-7 cells. These results clearly show that all particles are efficiently internalized (>75%) by MCF-7 cells regardless of the N/P ratio. Earlier research showed that increasing

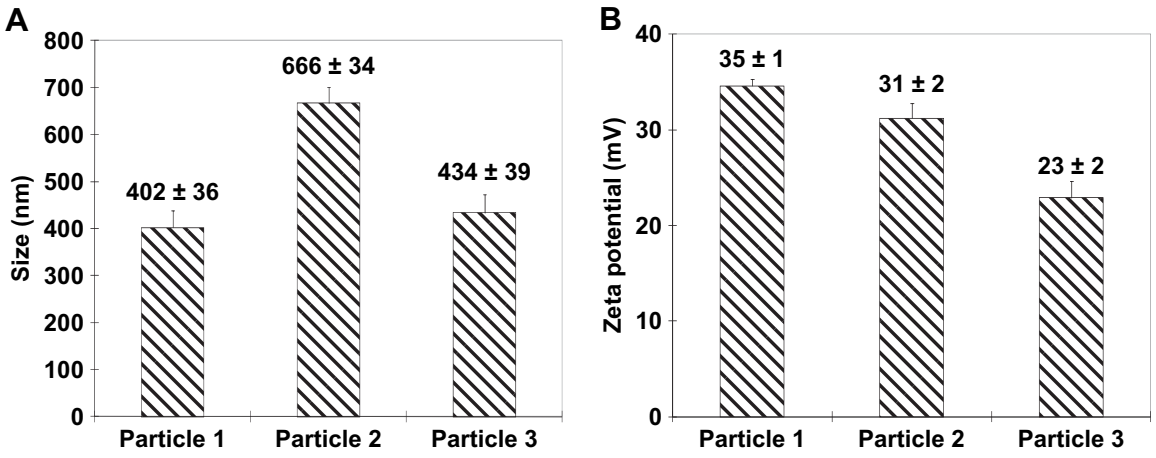

Fig. 11. The size (A) and zeta potential (B) of particles 1–3 prepared by complexation of poly(EAA-*co*-BMA)-b-NASI-g-(HMA-*co*-TMAEMA), poly(EAA-*co*-BMA)-b-Asp-g-(HMA-*co*-TMAEMA), and poly(EAA-*co*-HMA)-b-Asp-g-(HMA-*co*-TMAEMA) comb-like polymers with 0.57 μg of anti-GAPDH siRNA at a N/P (+/−) ratio of 2.5/1, respectively. The plotted results are the average + the standard error of the mean of two independent experiments each carried out in triplicates.

the particle's cationic nature is typically associated with toxicity [59,60] or low transfection efficiency due to poor decomplexation of the loaded DNA/RNA molecules [61,62]. Consequently, we decided to evaluate the transfection efficiency of the particles prepared at N/P ratio of 2.5/1, which will have the optimum number of cationic TMAEMA residues to complex the loaded siRNA molecules without inducing cellular toxicity or hindering the cytoplasmic decomplexation of the loaded siRNA.

3.7. Effect of "smart" particles on GAPDH expression

The ability of particles 1–3 to deliver functional siRNA molecules into the cytoplasm of MCF-7 breast cancer cells was assayed based on their ability to selectively knockdown GAPDH gene expression at the mRNA and protein levels. We utilized the kDalert assay kit to measure the changes in GAPDH protein level upon incubation with particles that encapsulate the anti-GAPDH siRNA molecules compared to those encapsulating a scrambled siRNA sequence. We utilized siPORT amine-based complexes encapsulating an equal dose of anti-GAPDH siRNA molecules as a positive control to determine the maximum level of knockdown that can be achieved using robust commercial transfection reagents.

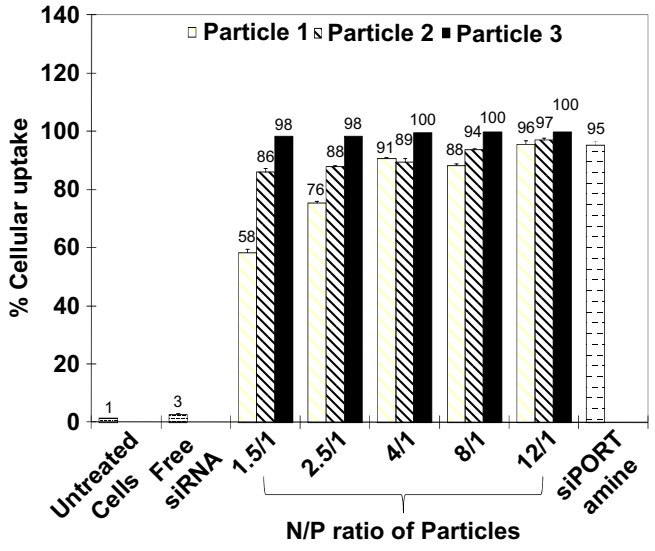

Fig. 12. The % of MCF-7 cells that internalized free siRNA molecules, particles 1–3, and siPORT amine-based complexes upon incubation for 6 h in a serum-free culture medium. Particles 1–3 were prepared by complexation of poly(EAA-*co*-BMA)-b-NASI-g-(HMA-*co*-TMAEMA), poly(EAA-*co*-BMA)-b-Asp-g-(HMA-*co*-TMAEMA), and poly (EAA-*co*-HMA)-b-Asp-g-(HMA-*co*-TMAEMA) comb-like polymers with 0.57 μg of fluorescently-labeled anti-GAPDH siRNA at different N/P (+/−) ratios, respectively. The plotted results are the average + the standard error of the mean of four independent experiments each carried out in triplicates.

Results show that particles 1, 2, and 3 caused 36%, 27%, and 20% reduction in GAPDH protein expression, respectively (Fig. 13A). Results also show that siPORT amine-based complexes produced 38% reduction in GAPDH protein expression. It is important to note that particle 2 caused non-specific reduction in GAPDH expression upon incubation with the particles that encapsulate scrambled siRNA molecules, which may be a result of polymer's toxicity towards MCF-7 cells. By comparing the activity of particles 1 and 3, it is clear that particle 1 is more efficient in silencing the expression of the targeted gene (GAPDH) reaching the same level of knockdown achieved by commercial transfection reagents without inducing any toxicity. The observed reduction in GAPDH protein levels was also evident at the mRNA level with particle 1 and siPORT amine-based complexes inducing 40% knockdown in GAPDH mRNA levels (Fig. 13B). The higher activity of particles 1 is a result of higher grafting efficiency (92.5%) and TMAEMA content per comb-like polymer compared to those used to prepare particles 2 and 3 (Table 1). These results collectively indicate that particle 1 is an effective carrier for intracellular delivery of therapeutic siRNA molecules.

We prepared a series of particle 1 by complexing poly(EAA-*co*-BMA)-b-NASI-g-(HMA-*co*-TMAEMA) comb-like polymers with siRNA molecules at different N/P ratios to determine the effect of particle composition on their ability to achieve functional knockdown of GAPDH expression in MCF-7 cells. Results show that particles prepared at N/P ratio of 1.5/1 failed to reduce GAPDH expression compared to those prepared at N/P ratio of 2.5/1, which reduced GAPDH expression by 36–40% at both the mRNA and protein levels (Fig. 14). Particles prepared at 4/1 and 8/1 N/P ratios reduced GPADH expression by ~25%, however their effect was associated with reduction in cell viability indicated by the non-specific decline in mRNA levels observed upon treatment with particles encapsulating scrambled siRNA sequences (Fig. 14B). These results are in agreement with earlier research clearly documenting the non-specific toxicity of particles with high content of

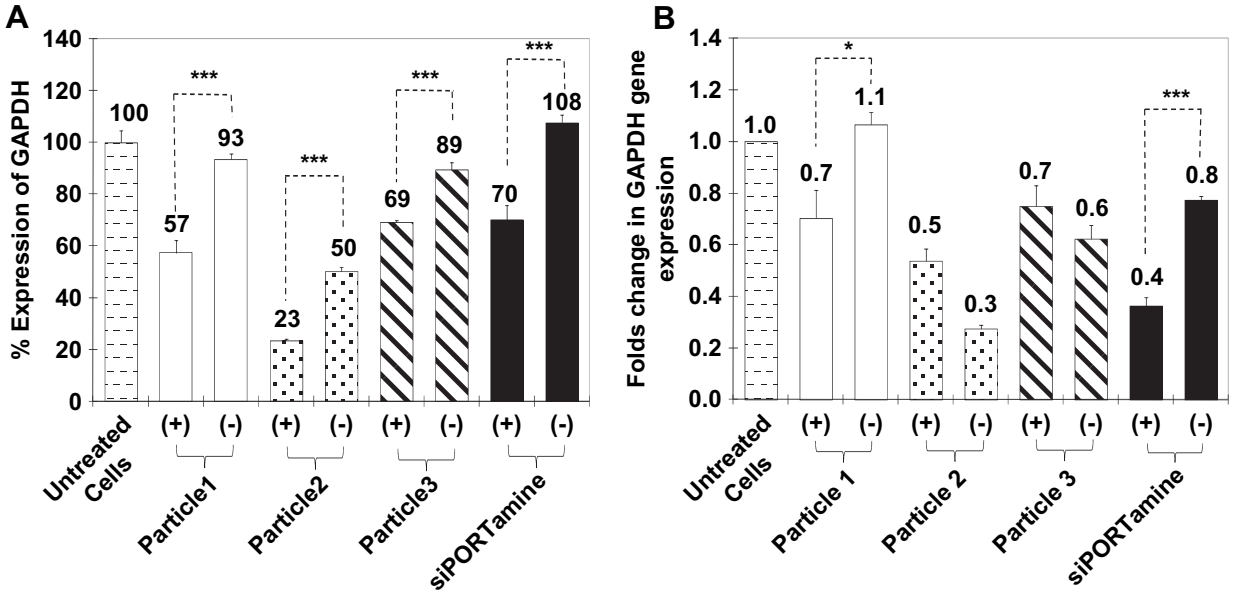

Fig. 13. The effect of particles 1–3 encapsulating 100 nM of anti-GAPDH siRNA (+) or a scrambled siRNA sequence (−) on GAPDH protein expression (A) and mRNA levels (B) in MCF-7 breast cancer cells. Particles 1–3 were prepared by complexation of poly(EAA-*co*-BMA)-b-NASI-g-(HMA-*co*-TMAEMA), poly(EAA-*co*-BMA)-b-Asp-g-(HMA-*co*-TMAEMA), and poly(EAA-*co*-HMA)-b-Asp-g-(HMA-*co*-TMAEMA) comb-like polymers with 0.57 μg of the selected siRNA sequence at a N/P (+/−) ratio of 2.5/1. The mRNA levels for GPADH gene are normalized to mRNA levels of β-actin. The plotted results are the average + the standard error of the mean of three independent experiments with five replicates for each treatment. Statistical difference between particles encapsulating anti-GAPDH siRNA (+) and scrambled siRNA sequence (−) was evaluated using paired *t* test where * denotes $p \leq 0.05$, ** denotes $p \leq 0.01$, and *** denotes $p \leq 0.005$.

cationic polymers [59,60,63–65]. These results further confirmed the potential of the particles prepared by complexation of poly (EAA-*co*-BMA)-b-NASI-g-(HMA-*co*-TMAEMA) comb-like polymers with therapeutic siRNA molecules at N/P ratio of 2.5/1 as effective carriers for intracellular delivery of nucleic acid drugs.

3.8. Effect of serum and nuclease enzymes on "smart" particles

Particles have to shield and protect their therapeutic cargo from serum proteins and nuclease enzymes, which proved to degrade DNA/RNA molecules into small ineffective fragments [60,66–68] to become therapeutically effective *in vivo*. We examined the effect of serum proteins on particles 1–3 prepared at a N/P ratio of 2.5/1 by incubating these particles with 10% and 25% FBS for 6 h at 37 °C and measuring the amount of siRNA released in solution using the PicoGreen dye. Results show that particles 1–3 retained 92–95% of the loaded siRNA molecules upon incubation in serum-free medium for 6 h (Fig. 15). However, incubation of these particles with 10–25% of FBS caused partial decomplexation of these particles and reduced the amount of shielded siRNA molecules to

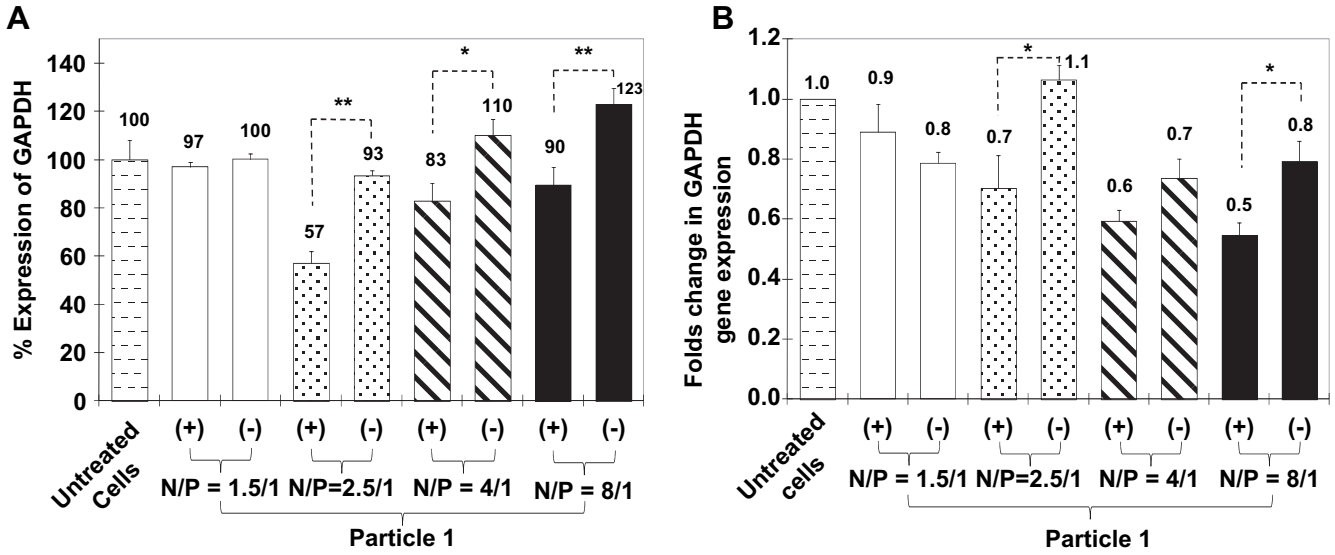

Fig. 14. The effect of particle 1 prepared by complexation of poly(EAA-*co*-BMA)-b-NASI-g-(HMA-*co*-TMAEMA) comb-like polymers with 0.57 μg of anti-GAPDH siRNA (+) or a scrambled siRNA sequence (−) at different N/P (+/−) ratios on GAPDH protein expression (A) and mRNA levels (B) in MCF-7 breast cancer cells. The plotted results are the average + the standard error of the mean of three independent experiments with five replicates for each treatment. Statistical difference between particles encapsulating anti-GAPDH siRNA (+) and scrambled siRNA sequence (−) was evaluated using paired *t* test where * denotes $p \leq 0.05$, ** denotes $p \leq 0.01$.

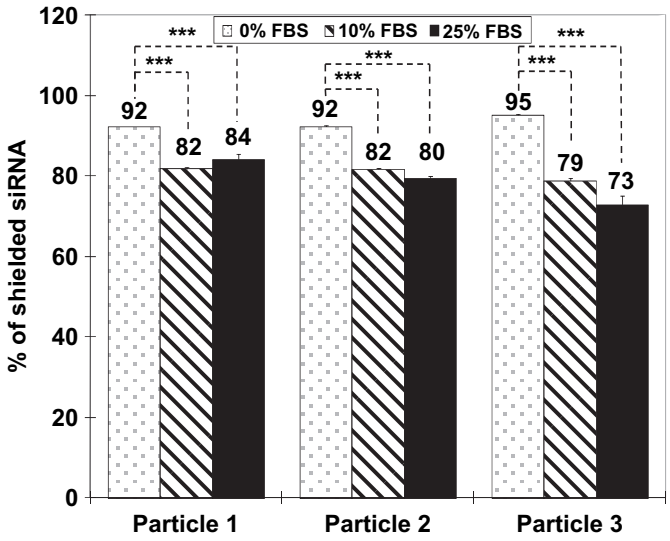

Fig. 15. The change in the amount of siRNA molecules encapsulated within particles 1–3 upon incubation for 6 h at 37 °C with 10% and 25% of fetal bovine serum (FBS) compared to the particles incubated in serum-free medium. SYBR Green II dye was used to measure the amount of free siRNA molecules present in each solution to determine siRNA leakage from each particle at different FBS concentrations. The amount of free siRNA molecules present in solution was normalized to the encapsulated siRNA dose (0.57 μg) to determine % of shielded siRNA in each particle under different conditions. All particles were prepared at N/P (+/−) ratio of 2.5/1. The plotted results are the average + the standard error of the mean of a single experiment carried out in triplicates. Statistical difference between particles incubated with 10% and 25 % FBS and those incubated in serum-free medium was evaluated using paired t test where *** denotes $p \leq 0.005$.

75–80% of the loaded siRNA molecules. Despite the partial release of 20–25% of the loaded siRNA molecules, these particles retained and shielded the bulk of the loaded dose at a low N/P ratio for a long incubation time.

We evaluated the stability of particle 1 prepared at different N/P ratios upon incubation with RNase V1 at 37 °C for 30 min using the standard gel retardation assay. By comparing the fluorescence intensity of the wells loaded with the particles treated with RNase enzyme (+) to those incubated with blank buffer (−) using Image J software, our results show that particle 1 prepared at N/P ratio of 2.5/1 and higher was able to retain and shield > 95% of the loaded siRNA molecules (Fig. 16). The particles prepared at N/P ratio of 1/1

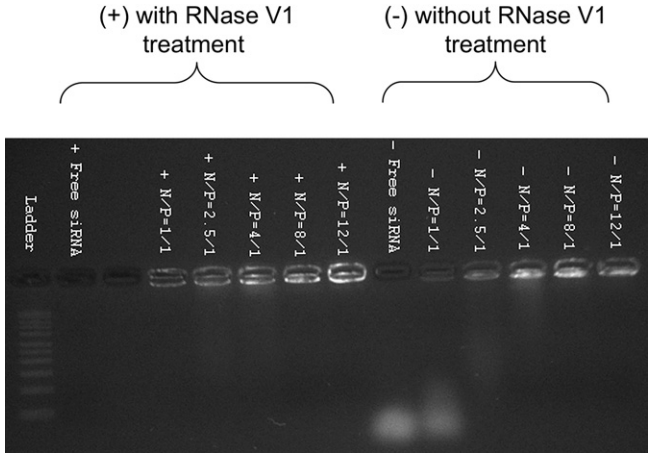

Fig. 16. Image of a 1% w/v agarose gel stained with SYBR Green II dye showing the electrophoretic mobility of free siRNA molecules (0.75 μg) and an equal amount complexed with poly(EAA-*co*-BMA)-b-NASI-g-(HMA-*co*-TMAEMA) comb-like polymer at different N/P (+/−) ratios upon incubation with RNase V1 enzyme (+) or blank buffer (−) for 30 min at 37 °C.

shielded the fraction of the siRNA molecules that is complexed with the polymeric carrier and entrapped into the loading well. The free fraction of siRNA molecules that appeared as a faint band with similar electrophoretic mobility to free siRNA was digested by the RNase enzyme (Fig. 16). These results collectively indicate that particles 1–3 retained and shielded > 75% of their siRNA cargo in presence of 25% (v/v) FBS and particle 1 protected > 95% of the loaded siRNA molecules in presence of nuclease enzymes at N/P ratio of 2.5/1 and higher, which indicate their potential as effective DNA/RNA carriers *in vivo*.

4. Conclusions

We have designed and synthesized a new series of degradable, pH-sensitive, membrane-destabilizing, comb-like polymers that exhibit a robust membrane-destabilizing activity in response to acidic pH gradients similar to those present in the endosome. These comb-like polymers proved to degrade into smaller fragments in acidic environment, which will minimize their toxicity and facilitate their *in vivo* elimination by renal excretion. These polymers successfully complexed model siRNA molecules into pH-sensitive, serum- and nuclease-stable particles at low N/P ratios, which indicate their ability to encapsulate large doses of therapeutic nucleic acids. Particles 1–3 proved to successfully delivery functional siRNA molecules into the cytoplasm of MCF-7 breast cancer cells and achieve targeted gene knockdown at both mRNA and protein levels with particle 1 being the most effective formulation. These results collectively indicate the potential of these particles particularly particle 1 to serve as a carrier for enhancing the intracellular delivery of therapeutic nucleic acids.

Acknowledgments

This research was supported in part by the U.S. Department of Defence Breast Cancer Research Program (Award #W81XWH-05-1-0240 to M. El-Sayed). Lisa Birrell was supported by the Marian Sarah Parker Scholarship and Edmunson Summer Fund.

Appendix. Supplementary data

Supplementary data associated with this article can be found in the on-line version, at doi:10.1016/j.biomaterials.2010.05.048.

Appendix

Figures with essential colour discrimination. Figs. 1, 2, 3, 6 and 12 in this article is difficult to interpret in black and white. The full color images can be found in the on-line version, at doi:10.1016/j.biomaterials.2010.05.048.

References

[1] deFougerolles A, Vornlocher H-P, Maraganore J, Lieberman J. Interfering with disease: a progress report on siRNA-based therapeutics. Nat Rev Drug Discov 2007;6(6):443–53.
[2] Hassan A. Potential applications of RNA interference-based therapeutics in the treatment of cardiovascular disease. Recent Pat Cardiovasc Drug Discov 2006;1(2):141–9.
[3] Koutsilieri E, Rethwilm A, Scheller C. The therapeutic potential of siRNA in gene therapy of neurodegenerative disorders. J Neural Transm Suppl 2007;72:43–9.
[4] Tili E, Michaille JJ, Gandhi V, Plunkett W, Sampath D, Calin GA. miRNAs and their potential for use against cancer and other diseases. Future Oncol 2007;3(5):521–37.
[5] Zhang J, Wu YO, Xiao L, Li K, Chen LL, Sirois P. Therapeutic potential of RNA interference against cellular targets of HIV infection. Mol Biotechnol 2007;37(3):225–36.
[6] Lechardeur D, Lukacs GL. Intracellular barriers to non-viral gene transfer. Curr Gene Ther 2002;2(2):183–94.

[7] Nielsen PE. Addressing the challenges of cellular delivery and bioavailability of peptide nucleic acids (PNA). Q Rev Biophys 2005;38(4):345–50.
[8] Jere D, Jiang HL, Arote R, Kim YK, Choi YJ, Cho MH, et al. Degradable polyethylenimines as DNA and small interfering RNA carriers. Expert Opin Drug Deliv 2009;6(8):827–34.
[9] Lai WF, Lin MC. Nucleic acid delivery with chitosan and its derivatives. J Control Release 2009;134(6):158–68.
[10] Midoux P, Pichon C, Yaouanc JJ, Jaffrès PA. Chemical vectors for gene delivery: a current review on polymers, peptides and lipids containing histidine or imidazole as nucleic acids carriers. Br J Pharmacol 2009;157 (2):166–78.
[11] Pangburn TO, Petersen MA, Waybrant B, Adil MM, Kokkoli E. Peptide- and aptamer-functionalized nanovectors for targeted delivery of therapeutics. J Biomech Eng 2009;131(7):74005–25.
[12] Grimm D, Kay MA. From virus evolution to vector revolution: use of naturally occurring serotypes of adeno-associated virus (AAV) as novel vectors for human gene therapy. Curr Gene Ther 2003;3:281–304.
[13] Cross KJ, Langley WA, Russell RJ, Skehel JJ, Steinhauer DA. Composition and functions of the influenza fusion peptide. Protein Pept Lett 2009;16 (7):766–78.
[14] Hughson FM. Structural characterization of viral fusion proteins. Curr Biol 1995;5:265–74.
[15] Ren J, Sharpe JC, Collier RJ, London E. Membrane translocation of charged residues at the tips of hydrophobic helices in the T domain of diphtheria toxin. Biochemistry 1999;38:976–84.
[16] Skehel JJ, Wiley DC. Receptor binding and membrane fusion in virus entry: the influenza hemagglutinin. Annu Rev Biochem 2000;69:531–69.
[17] Wiley DC, Skehel JJ. The structure and function of the hemagglutinin membrane glycoprotein of influenza virus. Annu Rev Biochem 1987;56:365–94.
[18] Fattal E, Nir S, Parente RA, Szoka Jr FC. Pore-forming peptides induce rapid phospholipid flip-flop in membranes. Biochemistry 1994;33 (21):6721–31.
[19] Funhoff AM, Nostrum CFV, Lok MC, Kruijtzer JA, Crommelin DJ, Hennink WE. Cationic polymethacrylates with covalently linked membrane destabilizing peptides as gene delivery vectors. J Control Release 2005;101 (1–3):233–46.
[20] Lee H, Jeong JH, Park TG. A new gene delivery formulation of polyethylenimine/DNA complexes coated with PEG conjugated fusogenic peptide. J Control Release 2001;76(1–2):183–92.
[21] Li W, Nicol F, Szoka Jr FC. GALA: a designed synthetic pH-responsive amphipathic peptide with applications in drug and gene delivery. Adv Drug Deliv Rev 2004;56(7):967–85.
[22] Parente RA, Nadasdi L, Subbarao NK, Szoka Jr FC. Association of a pH-sensitive peptide with membrane vesicles: role of amino acid sequence. Biochemistry 1990;29(37):8713–9.
[23] Parente RA, Nir S, Szoka Jr FC. pH-dependent fusion of phosphatidylcholine small vesicles. Induction by a synthetic amphipathic peptide. J Biol Chem 1988;263(10):4724–30.
[24] Parente RA, Nir S, Szoka Jr FC. Mechanism of leakage of phospholipid vesicle contents induced by the peptide GALA. Biochemistry 1990;29 (37):8720–8.
[25] Plank C, Oberhauser B, Mechtler K, Koch C, Wagner E. The influence of endosome-disruptive peptides on gene transfer using synthetic virus-like gene transfer systems. J Biol Chem 1994;269:12918–24.
[26] Subbarao NK, Parente RA, Szoka Jr FC, Nadasdi L, Pongracz K. pH-dependent bilayer destabilization by an amphipathic peptide. Biochemistry 1987;26 (11):2964–72.
[27] El-Sayed MEH, Hoffman AS, Stayton PS. Smart polymeric carriers for enhanced intracellular drug delivery of therapeutic macromolecules. Expert Opin Biol Ther 2005;5(1):23–32.
[28] Yessine MA, Leroux JC. Membrane-destabilizing polyanions: interaction with lipid bilayers and endosomal escape of biomacromolecules. Adv Drug Deliv Rev 2004;56(7):999–1021.
[29] Thomas JL, Barton SW, Tirrell DA. Membrane solubilization by a hydrophobic polyelectrolyte: surface activity and membrane binding. Biophys J 1994;67:1101–6.
[30] Thomas JL, Tirrell DA. Polyelectrolyte-sensitized phospholipid vesicles. Acc Chem Res 1992;25:336–42.
[31] Murthy N, Chang I, Stayton PS, Hoffman AS. pH-sensitive hemolysis by random copolymers of alkyl acrylates and acrylic acid. Macromol Symp 2001;172:49–55.
[32] Murthy N, Robichaud JR, Tirrell DT, Stayton PS, Hoffman AS. The design and synthesis of polymers for eukaryotic membrane disruption. J Control Release 1999;61:137–43.
[33] Cheung CY, Murthy N, Stayton PS, Hoffman AS. A pH-sensitive polymer that enhances cationic lipid-mediated gene transfer. Bioconjug Chem 2001;12:906–10.
[34] Kiang T, Bright C, Cheung CY, Stayton PS, Hoffman AS, Leong KW. Formulation of chitosan-DNA nanoparticles with poly(propyl acrylic acid) enhances gene expression. J Biomater Sci Polym Ed 2004;15(11):1405–21.
[35] Kyriakides TR, Cheung CY, Murthy N, Bornstein P, Stayton PS, Hoffman AS. pH-Sensitive polymers that enhance intracellular drug delivery *in vivo*. J Control Release 2002;78:295–303.
[36] Cheung CY, Stayton PS, Hoffman AS. Poly(propylacrylic acid)-mediated serum stabilization of cationic lipoplexes. J Biomater Sci Polym Ed 2005;16 (2):163–79.
[37] Bulmus V, Woodward M, Lin L, Murthy N, Stayton PS, Hoffman AS. A new pH-responsive and glutathione-reactive, endosomal membrane-disruptive polymeric carrier for intracellular delivery of biomolecular drugs. J Control Release 2003;93:105–20.
[38] El-Sayed MEH, Hoffman AS, Stayton PS. Rational design of composition and activity correlations for pH-sensitive and glutathione-reactive polymer therapeutics. J Control Release 2005;101(1–3):47–58.
[39] Ferrito MS, Tirrell DA. Poly(2-ethylacrylic acid). Macromol Synth 1992;11:59–62.
[40] Lai JT, Filla D, Shea R. Functional polymers from novel carboxyl-terminated trithiocarbonates as highly efficient RAFT agents. Macromolecules 2002;35:6754–6.
[41] Yokoyama M, Okano T, Sakurai Y, Ekimoto H, Shibazaki C, Kataoka K. Toxicity and antitumor activity against solid tumors of micelle-forming polymeric anticancer drug and its extremely long circulation in blood. Cancer Res 1991;51:3229–36.
[42] Etrych T, Chytil P, Jelínková M, Říhová B, Ulbrich K. Synthesis of HPMA copolymers containing doxorubicin bound via a hydrazone linkage. Effect of spacer on drug release and *in vitro* cytotoxicity. Macromol Biosci 2002;2:43–52.
[43] Etrych T, Strohalm J, Kovár L, Kabesová M, Ríhová B, Ulbrich K. HPMA copolymer conjugates with reduced anti-CD20 antibody for cell-specific drug targeting. I. Synthesis and *in vitro* evaluation of binding efficacy and cytostatic activity. J Control Release 2009;140(1):18–26.
[44] Kovár M, Kovár L, Subr V, Etrych T, Ulbrich K, Mrkvan T, et al. HPMA copolymers containing doxorubicin bound by a proteolytically or hydrolytically cleavable bond: comparison of biological properties *in vitro*. J Control Release 2004;99(2):301–14.
[45] Krakovicová H, Etrych T, Ulbrich K. HPMA-based polymer conjugates with drug combination. Eur J Pharm Sci 2009;37(3–4):405–12.
[46] Kratz F, Beyer U, Schutte MT. Drug–polymer conjugates containing acid-cleavable bonds. Crit Rev Ther Drug Carrier Syst 1999;16:245–88.
[47] Říhová B, Etrych T, Pechar M, Jelínková M, Šťastný M, Hovorka O, et al. Doxorubicin bound to a HPMA copolymer carrier through hydrazone bond is effective also in a cancer cell line with a limited content of lysosomes. J Control Release 2001;74:225–32.
[48] Ulbrich K, Etrych T, Chytil P, Jelínková M, Říhová B. Antibody-targeted polymer-doxorubicin conjugates with pH-controlled activation. J Drug Target 2004;12(8):477–89.
[49] Kale AA, Torchilin VP. Design, synthesis, and characterization of pH-sensitive PEG-PE conjugates for stimuli-sensitive pharmaceutical nanocarriers: the effect of substitutes at the hydrazone linkage on the pH stability of PEG-PE conjugates. Bioconjug Chem 2007;18(2):363–70.
[50] Kale AA, Torchilin VP. Enhanced transfection of tumor cells *in vivo* using "Smart" pH-sensitive TAT-modified pegylated liposomes. J Drug Target 2007;15(7–8):538–45.
[51] Kale AA, Torchilin VP. "Smart" drug carriers: PEGylated TATp-modified pH-sensitive liposomes. J Liposome Res 2007;17(3–4):197–203.
[52] Sawant RM, Hurley JP, Salmaso S, Kale A, Tolcheva E, Levchenko TS, et al. "SMART" drug delivery systems: double-targeted pH-responsive pharmaceutical nanocarriers. Bioconjug Chem 2006;17:943–9.
[53] Hruby M, Kucka J, Lebeda O, Mackova H, Babic M, Konak C, et al. New bioerodable thermoresponsive polymers for possible radiotherapeutic applications. J Control Release 2007;119(1):25–33.
[54] Sonawane ND, Szoka Jr FC, Verkman AS. Chloride accumulation and swelling in endosomes enhances DNA transfer by polyamine-DNA polyplexes. J Biol Chem 2003;278(45):44826–31.
[55] Murthy N, Campbell J, Fausto N, Hoffman AS, Stayton PS. Bioinspired pH-responsive polymers for the intracellular delivery of biomolecular drugs. Bioconjug Chem 2003;14:412–9.
[56] Murthy N, Campbell J, Fausto N, Hoffman AS, Stayton PS. Design and synthesis of pH-responsive polymeric carriers that target uptake and enhance the intracellular delivery of oligonucleotides. J Control Release 2003;89 (3):365–74.
[57] Palermo EF, Kuroda K. Chemical structure of cationic groups in amphiphilic polymethacrylates modulates the antimicrobial and hemolytic activities. Biomacromolecules 2009;10(6):1416–28.
[58] Yuan F, Dellian M, Fukumura D, Leunig M, Berk DA, Torchilin VP, et al. Vascular permeability in a human tumor xenograft: molecular size dependence and cutoff size. Cancer Res 1995;55(17):3752–6.
[59] Oskuee RK, Dehshahri A, Shier WT, Ramezani M. Alkylcarboxylate grafting to polyethylenimine: a simple approach to producing a DNA nanocarrier with low toxicity. J Gene Med 2009;11(10):921–32.
[60] Wen Y, Pan S, Luo X, Zhang X, Zhang W, Feng M. A biodegradable low molecular weight polyethylenimine derivative as low toxicity and efficient gene vector. Bioconjug Chem 2009;20(2):322–32.
[61] Gabrielson NP, Pack DW. Acetylation of polyethylenimine enhances gene delivery via weakened polymer/DNA interactions. Biomacromolecules 2006;7:2427–35.
[62] Kabanov AV, Kabanov VA. DNA complexes with polycations for the delivery of genetic material into cells. Bioconjug Chem 1995;6(1):7–20.

[63] Brownlie A, Uchegbu IF, Schätzlein AG. PEI-based vesicle-polymer hybrid gene delivery system with improved biocompatibility. Int J Pharm 2004;274 (1–2):41–52.
[64] Deng R, Yue Y, Jin F, Chen Y, Kung HF, Lin MC, et al. Revisit the complexation of PEI and DNA – how to make low cytotoxic and highly efficient PEI gene transfection non-viral vectors with a controllable chain length and structure? J Control Release 2009;140(1):40–6.
[65] Gebhart CL, Kabanov AV. Evaluation of polyplexes as gene transfer agents. J Control Release 2001;73(2–3):401–16.
[66] Konopka K, Overlid N, Nagaraj AC, Düzgüneş N. Serum decreases the size of Metafectene-and Genejammer-DNA complexes but does not affect significantly their transfection activity in SCCVII murine squamous cell carcinoma cells. Cell Mol Biol Lett 2006;11(2):171–90.
[67] Merdan T, Kunath K, Petersen H, Bakowsky U, Voigt KH, Kopecek J, et al. PEGylation of poly(ethylene imine) affects stability of complexes with plasmid DNA under *in vivo* conditions in a dose-dependent manner after intravenous injection into mice. Bioconjug Chem 2005;16(4):785–92.
[68] Liu Y, Reineke TM. Poly(glycoamidoamine)s for gene delivery: stability of polyplexes and efficacy with cardiomyoblast cells. Bioconjug Chem 2006;17(1):101–8.